



A new incubation system to simultaneously measure N₂ as well as N₂O and CO₂ fluxes from plant-soil mesocosms

Irina Yankelzon¹ · Georg Willibald¹ · Michael Dannenmann¹ · Francois Malique¹ · Ulrike Ostler¹ · Clemens Scheer¹ · Klaus Butterbach-Bahl^{1,2}

Received: 15 November 2023 / Revised: 26 February 2024 / Accepted: 27 February 2024
© The Author(s) 2024, corrected publication 2024

Abstract

This study presents a novel plant-soil mesocosm system designed for cultivating plants over periods ranging from days to weeks while continuously measuring fluxes of N₂, N₂O and CO₂. For proof of concept, we conducted a 33-day incubation experiment using six soil mesocosms, with three containing germinated wheat plants and three left plant-free. To validate the magnitude of N₂ and N₂O fluxes, we used ¹⁵N-enriched fertilizer and a ¹⁵N mass balance approach. The system inherent leakage rate was about 55 μg N m⁻² h⁻¹ for N₂, while N₂O leakage rates were below the detection limit (< 1 μg N m⁻² h⁻¹). In our experiment, we found higher cumulative gaseous N₂+N₂O losses in sown soil (0.34 ± 0.02 g N m⁻²) as compared to bare soil (0.23 ± 0.01 g N m⁻²). N₂ fluxes accounted for approximately 94–96% of total gaseous N losses in both planted and unplanted mesocosms. N losses, as determined by the ¹⁵N mass balance approach, were found to be 1.7 ± 0.5 g N m⁻² for the sown soil and 1.7 ± 0.6 g N m⁻² for the bare soil, indicating an inconsistency between the two assessment methods. Soil respiration rates were also higher in sown mesocosms, with cumulative soil and aboveground biomass CO₂ respiration reaching 4.8 ± 0.1 and 4.0 ± 0.1 g C m⁻² over the 33-day incubation period, in sown and bare soil, respectively. Overall, this study measured the effect of wheat growth on soil denitrification, highlighting the sensitivity and utility of this advanced incubation system for such studies.

Keywords Denitrification · N₂ emissions · Plant-soil mesocosms · He atmosphere system · Soil core method · Plants effect

Introduction

Measuring dinitrogen (N₂) production in soils due to denitrification remains one of the largest challenges in ecosystem biogeochemistry (Groffman et al. 2007). Understanding this process is critical for accurately assessing nitrogen (N) budgets in terrestrial ecosystems and their contribution to global N cycling. Denitrification is the sequential, stepwise microbial respiratory reduction of oxidized forms of inorganic nitrogen (N), such as nitrate (NO₃⁻) or nitrite (NO₂⁻),

to nitric oxide (NO), nitrous oxide (N₂O), and the terminal product N₂. Denitrification is the dominating process removing reactive nitrogen (N_r) from the terrestrial biosphere and returning it to the atmosphere in the inert form of N₂. Depending on its product stoichiometry, denitrification can be regarded as both an environmentally beneficial and a detrimental process. On the one hand, denitrifying bacteria reduce NO₃⁻ to the inert gas N₂, thus preventing excessive losses of N_r into the environment, where it may cause eutrophication of surface waters (Galloway et al. 2002), biodiversity depletion (Bobbink et al. 1998), alter net primary production and nutrient cycling (Vitousek et al. 1997), or jeopardize human health due to drinking water contamination (Wolfe and Patz 2002). On the other hand, during the process of denitrification, significant quantities of trace gases, namely N₂O and NO, are generated. These gases have considerable importance as both primary and secondary greenhouse gases, and they play a significant role in atmospheric chemistry dynamics (Fowler et al. 2009).

✉ Klaus Butterbach-Bahl
klaus.butterbach-bahl@kit.edu

¹ Karlsruhe Institute of Technology, Institute for Meteorology and Climate Research (IMK-IFU),
82467 Garmisch-Partenkirchen, Germany

² Pioneer Center Land-CRAFT, Dept. Agroecology, University of Aarhus, Aarhus, Denmark

Denitrification is the major N loss process in soils, and its product ratio, specifically the $N_2O/(N_2 + N_2O)$ ratio, significantly influences its environmental impacts (Kuenen and Robertson 1994). This product ratio of denitrification is known to be influenced by various factors, including oxygen (O_2) availability (Firestone and Tiedje 1979), as well as the availability of N and carbon (C) in the soil (Chen et al. 2019; Qin et al. 2017). Additionally, soil pH (Šimek and Cooper 2002), the microbial community composition (Cavigelli and Robertson 2000) and copper availability (Shen et al. 2020) play significant roles in shaping the denitrification product ratio. As an anaerobic process, denitrification mostly occurs at anoxic microsites in unsaturated soils, and as soil O_2 availability increases, it becomes less prevalent. To perform heterotrophic microbial denitrification, readily available C as an alternative electron donor is required with the majority of C originating from decomposing plant litter (aboveground or belowground) or from exudation by plant roots (Weier et al. 1993). Hence, plant-derived C has been shown to stimulate microbial activity and denitrification (Grayston et al. 1997; Malique et al. 2019). However, direct C supply to denitrifiers is not the sole pathway of how plants are affecting denitrification. For example, root respiration and stimulated microbial respiration create O_2 -depleted soil microsites that shape the ecological niches for denitrification (Bakken 1988; Hayashi et al. 2015). In contrast, interspecies competition for NO_3^- between plants and denitrifiers within the rhizosphere may also lead to a decrease in soil denitrification activity (Kuzyakov and Xu 2013; LeBauer and Treseder 2008).

Other mechanisms by which plants influence the soil denitrification activity are related to variations in the soil redox potential, e.g., due to a) radial O_2 losses by roots of wetland plants (Butterbach-Bahl et al. 2000; Sutton-Grier et al. 2013), or due to plant soil water uptake, which affects soil moisture and consequently soil aeration and the occurrence of anoxic microsites in soils (Bakken 1988; Von Rheinbaben and Trolldenier 1984).

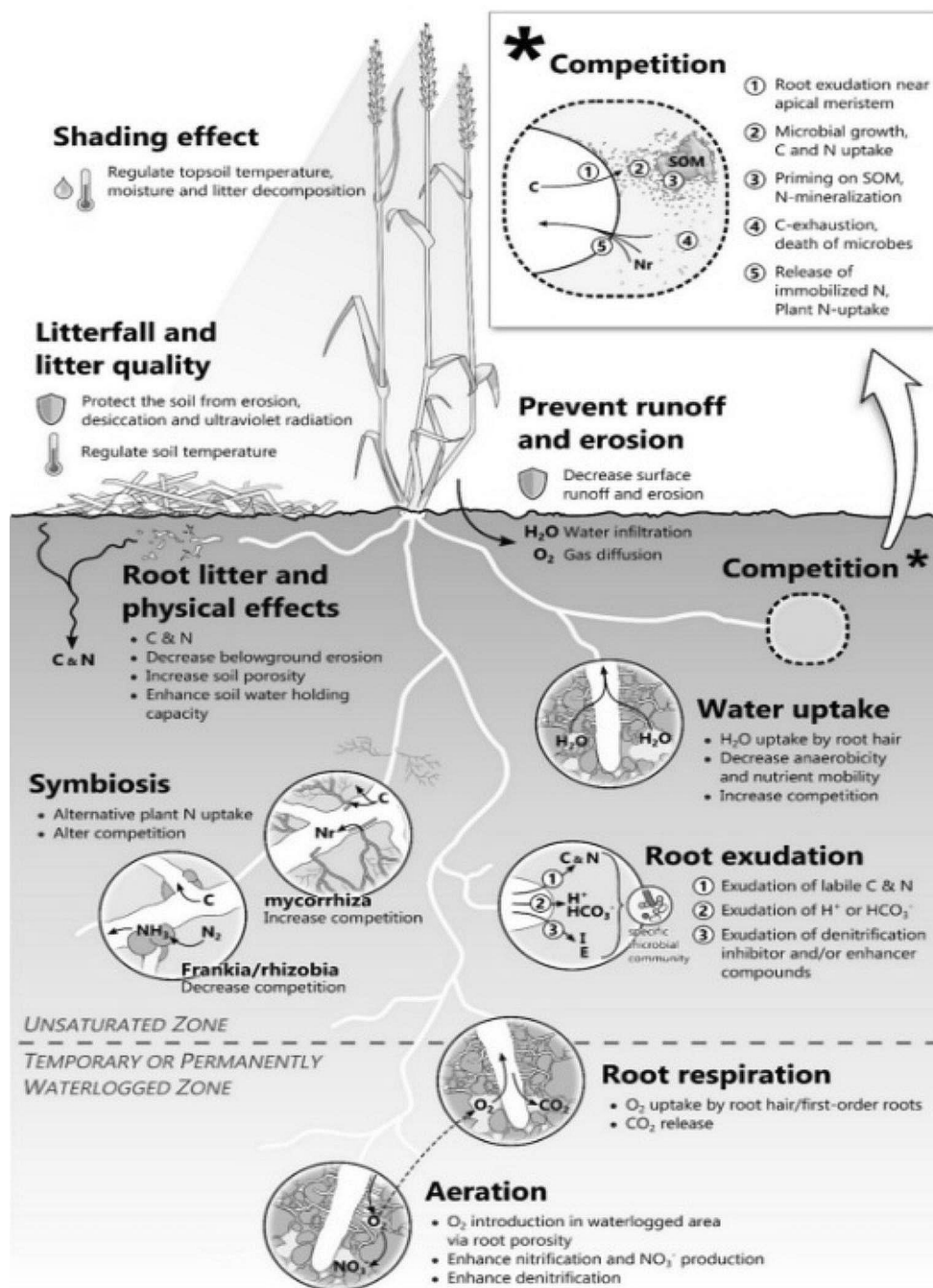
Given the ecological importance of denitrification and the obvious role plants may play in controlling soil denitrification activities (Fig. 1), rather little is known about the extent to which plants may affect rhizosphere denitrification. This is due to the persistent and mostly unresolved methodological challenges in measuring comparably small soil N_2 fluxes from denitrification given the atmospheric background level of N_2 which stands at 78%. This methodological issue limits our understanding of the impact of one of the most important sinks for N_f and also hampers the quantification, understanding, and biogeochemical modeling of the denitrification process as a whole (Boyer and Howarth 2008; Groffman et al. 2007, 2009).

There are several methods for estimating denitrification and gaseous N losses from the soil. These methods are based on (a) acetylene (C_2H_2) inhibition (Yoshinari et al. 1977); (b) stable isotope tracing techniques, such as direct $^{15}N_2$ flux measurements upon addition of $^{15}NO_3^-$ (Kulkarni et al. 2014), ^{15}N mass balance (Zhou et al. 2016), isotope dilution (Wessel and Tietema 1992), and isotope fractionation (Mariotti et al. 1981); (c) non-labeled N mass balance approaches (e.g., Jossette et al. 1999). Additionally, in the past two decades, the Helium (He) gas flow soil core technique has emerged as a direct measurement method. This technique enables the direct measurement of N_2 production in an N_2 -free environment without the need for chemical or tracer additions, integrating production across all source processes, including microbial and abiotic processes (Butterbach-Bahl et al. 2013; Chen et al. 2015). The method is based on the establishment of an N_2 -free He/ O_2 atmosphere in an extremely gastight soil incubation system so that accumulation of N_2 (as well as N_2O and NO) from all source processes can be measured over time (Burgin et al. 2010; Burgin and Groffman 2012; Butterbach-Bahl et al. 2002; Dannenmann et al. 2008; Scholefield et al. 1997; Wang et al. 2011). Measurements based on the He gas flow soil core technique have shown that total denitrification and N_2 losses from terrestrial ecosystems have been underestimated previously (Burgin and Groffman 2012; Butterbach-Bahl et al. 2013; Kulkarni et al. 2014; Scheer et al. 2020).

There is a wide range of studies focusing on He gas flow soil core measurements. These studies have employed both static (Butterbach-Bahl et al. 2002; Wang et al. 2011) and dynamic chamber approaches (Fiedler et al. 2017; Lewicka-Szczebak and Well 2020) for measuring N_2 fluxes from soil cores. The static approach involves no continuous He/ O_2 flow through the chamber headspace, while the dynamic approach maintains a continuous He/ O_2 flow through the chamber headspace.

The size of soil cores used in these measurements also varies significantly. Some studies have utilized small cores (e.g., 5.6 cm diameter and 4 cm height) incubated in sets within the same incubation vessel to address spatial variability (Dannenmann et al. 2011). Other studies have utilized rather large soil columns (e.g., 12.5 cm diameter and 15 cm height) (Butterbach-Bahl et al. 2002; Scheer et al. 2009). However, despite the advances in these techniques, the primary focus of these studies was on disentangling the effects of soil environmental conditions on microbial N turnover processes and denitrification products, while potential impacts of plants on rhizosphere processes and denitrification remained largely unexplored. Understanding the role of plants in denitrification is crucial for comprehending the complete picture of this essential N cycling process in terrestrial ecosystems. One of the main limitations of

Fig. 1 Plant mechanisms directly or indirectly affecting rhizosphere denitrification



these systems is their opacity and small size, which hinders the growth of significant biomass (although there are a few studies that have included plants in dark chambers, e.g., Zistl-Schlingmann et al. 2019). Overcoming the drawbacks of such a system requires significant engineering efforts, and any improvement, such as increasing the headspace volume to allow for plant growth, may negatively affect the detection limit for N₂ fluxes. Additionally, maintaining steady CO₂ levels in the headspace during day and night

light cycles becomes challenging when including growing plants in the setup.

However, recent research conducted with a new continuous-flow He/O₂ incubation system demonstrated that the root system of a growing barley plant induces increased losses of both N₂O and N₂ through denitrification, emphasizing the importance of further research on the plant effects on denitrification (Senbayram et al. 2020).

In this study, our primary objective was to develop a plant-soil mesocosm system based on the He gas flow soil

core technique, enabling the cultivation of plants over periods ranging from days to weeks while continuously measuring N_2 , N_2O , and CO_2 fluxes. Additionally, we aimed to validate our direct measurements of N gas loss by establishing a full N mass balance based on the application of ^{15}N enriched fertilizer to the mesocosms. We hypothesized that by comparing planted and bare soil, the newly developed system would reveal an increase in N_2 losses by denitrification associated with the growth of plant biomass, thus demonstrating the influence of plants on soil denitrification processes. In the following sections, we will provide a comprehensive description of the newly constructed plant-soil mesocosm system, highlighting its capabilities and detection limits. Furthermore, we will present the results of an experiment demonstrating the functionality of the system functionality with and without plants, as well as a comparison of the gaseous $N_2 + N_2O$ losses with this approach with the results derived using a ^{15}N mass balance approach.

Methods

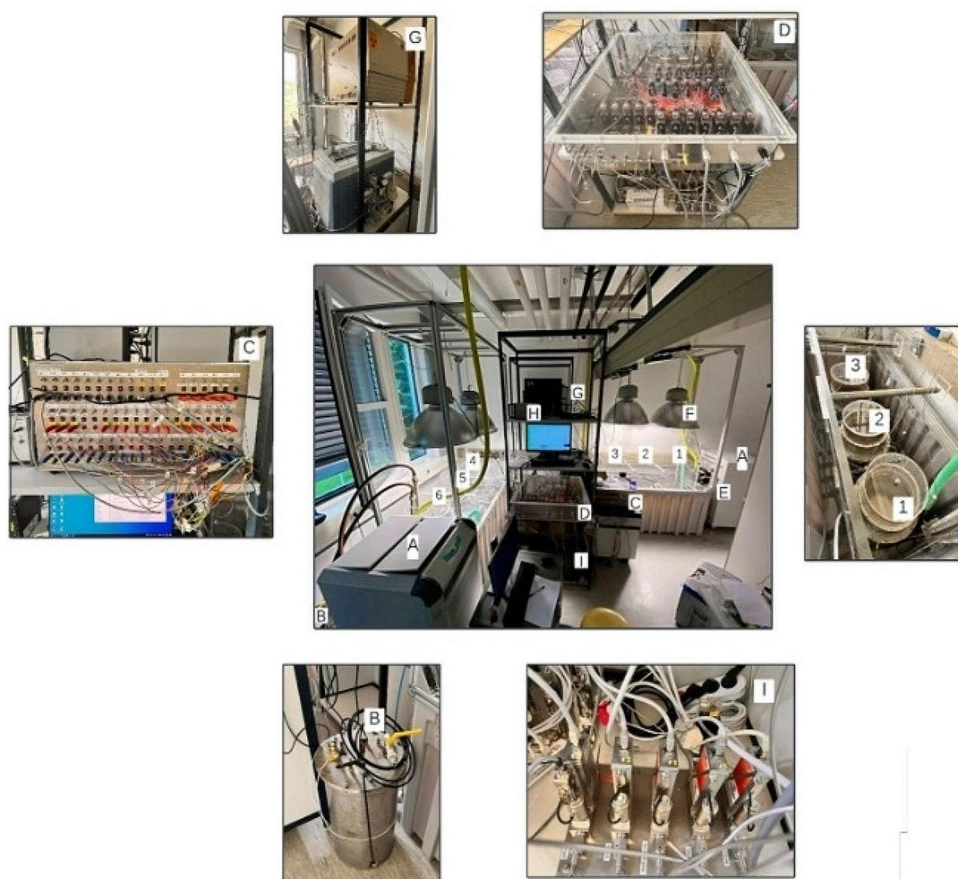
System setup and general system functioning

The newly developed system for simultaneous and continuous measurement of N_2 , N_2O , and CO_2 fluxes from plant-soil mesocosms is illustrated in Fig. 2. The system is comprised of six gastight mesocosms, with the top part of the chambers being translucent to allow illumination of plants with light sources. Additionally, the system includes gas flow controllers, a steering unit responsible for regulating and automating the sampling from the mesocosms' headspace, and analyzers for determining gas concentrations. To maintain temperature control, the mesocosms are placed in thermostatic water baths. Furthermore, the mesocosms can be irrigated with N_2 -free water sourced from a He-flushed water tank.

To ensure the utmost gas-tightness for the entire system, we utilized stainless-steel materials and leak-tight connectors for various components, including switching valves, flow controllers, tubing, and connectors. For enhanced

Fig. 2 Photos of the plant-soil incubation system. 1–6: transparent vessels for incubation of plant-soil-mesocosms in He/ O_2 atmosphere, placed into a water bath. (a) temperature regulation of water; (b) He-flushed water tank containing irrigation/fertigation water; (c) electronic system control unit; (d) sampling unit- valves, gas mixing devices and sample loops, placed in He flushed box to avoid intrusion of atmospheric N_2 ; (e) water level regulating pump; (f) light sources; (g) gas chromatographs (PDHID for N_2 and GC-ECD for N_2O detection); (h) read-out-device for soil O_2 sensors; (i) flow controllers for different available gases and gas mixtures

The novel incubation system for simultaneous measurement of N_2 , N_2O , and CO_2 Fluxes from Plant-Soil Mesocosms:



sensitivity, critical parts such as switching valves were enclosed within a He-flushed controller box. During the N₂ removal period, the chambers function as a dynamic throughflow system, pushing the N₂-free gas mixture through the soil and headspace. However, during the measuring periods, the system offers flexibility and can be used in two modes: a static chamber mode (with no throughflow) where fluxes are determined based on changes in headspace gas concentrations over time, or a semi-dynamic chamber mode where flux estimates are derived from differences in inflow and outflow gas concentrations.

Here we will delve into each of the system's major components. A detailed description of the system, including the scheme of tubing and valves, can be found in the Supporting Information.

Mesocosms and gas exchange procedure

The empty mesocosm vessel, illustrated in Fig. S1 (Supplementary Information), consists of an external base chamber constructed of stainless steel. Inside this base chamber, another removable stainless-steel pot can be placed to hold the soil. A transparent Plexiglas top chamber, which also has a stainless-steel base, is installed on top of the stainless-steel base to allow for the illumination of growing plants. The connections between the incubation vessels and their transparent lids have dual sealings made of high-quality seals, O-Ring (Dichtelemente arcus GmbH, Germany) and the space between the sealings is flushed with He gas. The base chamber volume is 20.5 l, while the top Plexiglas chamber has a volume of 16.275 l, though the lid height can be adjusted as per experimental requirements.

The external base chamber permits the connection of various environmental sensors, such as O₂, CO₂, soil moisture, and temperature sensors. With the option for illumination, the system enables the study of the effects of day/night light cycles on soil-plant processes and the associated gas exchange. Lamps for illumination are installed directly above the water bath containing the mesocosms, providing a light intensity of approximately 1300 $\mu\text{mol m}^{-2} \text{s}^{-1}$ at the top of the vessel and about 630 $\mu\text{mol m}^{-2} \text{s}^{-1}$ at the soil surface (Fig. 2f). The entire mesocosm system is placed in a thermostatic water bath.

The external base chamber allows for two flushing modes: soil flushing and sealing flushing (Fig. S2). For soil flushing, there is an inlet for the flushing gas and an outlet located on the top of the Plexiglas lid. When soil flushing is initiated, the flushing gas enters the external base chamber and permeates throughout it. The gas then thoroughly flushes the soil within the inner pot through the porous glass until it reaches the top outlet, where the flushed soil gases are evacuated.

In the headspace flushing mode, the gas mixture enters the vessel's headspace through an inlet on the stainless base of the top Plexiglas chamber and flows out on the opposite side of the chamber.

Gas flow rates and controllers

Flow controllers (F-201CM, Bronkhorst, Germany) are used to regulate the inflow and outflow of gases in the system (Fig. 2i). Each vessel's headspace flow rates are individually controlled by a flow controller. The gas mixture provided to each vessel is controlled by a gas titration unit (FlowView 1.23, Bronkhorst, Germany), which allows for the precise mixing of He, O₂, and calibration gases at various concentrations.

For soil flushing, a predetermined mixture of O₂ and He gases, commonly in an 80–20% ratio, is used. The soil flushing rate is typically maintained at 500 ml min⁻¹. The process involves alternating periods of flushing and testing, and it takes approximately 48 h to achieve a soil atmosphere devoid of N₂, which is in agreement with methodological approaches used in earlier studies with soil-only mesocosm systems (e.g., Wang et al. 2011).

For gas flux measurements, the soil flushing is stopped and the system is switched to headspace flushing. The flow rate through the headspace can be adjusted, but it is usually set between 20 and 40 ml min⁻¹. Each of the six vessels is flushed and sampled individually in a predetermined sequence, and the complete sampling sequence for all six vessels takes approximately two hours.

Control of gas flow pathways

The steering unit (Fig. 2d) comprises a valve system that controls the gas flows to and from each individual vessel. It includes six valves for soil flushing (one per vessel), six valves for soil flushing outlets, six valves for headspace flushing, six headspace outlet valves, and one restrictor for the headspace calibration gas (Fig. S3). From the vessel headspace, the gases flow to a 10-port-flowthrough valve. This valve alternates between directing sample gas from one of the gas lines to the detectors and discharging gas from the other gas lines into the steering box.

The electronic steering unit (Fig. 2c) covers several power supply components for valves and sensors. Additionally, the unit provides the starting signal for the gas chromatograph analyzer. It also includes various modules (ICP modules, 7000 series) for signal conversion from sensors, such as moisture and temperature probes, for further experiments.

The unit is connected to custom-made software (Integrated Data Acquisition Software (IDAS), IMK-IFU,

Garmisch-Partenkirchen, Germany) for data acquisition and valve switching.

Gas analysis

Concentrations of N_2O in the gas stream are analyzed using a GC 17 A equipped with an electron capture detector (ECD) (Shimadzu, Germany). For N_2 analysis, a Thermo Scientific GC with a Pulsed Discharge Helium Ionization Detector (PDHID) (Vici AG, Switzerland), is used. Carbon dioxide concentrations are measured by probes (VAISALA GMP 252, Finland) placed in the gas stream directed towards the ECD detector. Peak integration for N_2O is carried out using the software PeakSimple (SRI Instruments, Torrance, USA), while N_2 peak integration is done with the Chromeleon software (Thermo Fisher Scientific, version 7.2).

Irrigation

For supplying vessels with irrigation water, a He-flushed water tank is utilized (Fig. S4). The tank is filled with water through the water inlet up to the level of the inside tube of the He outlet. During filling, the He outlet remains open. To remove N_2 from the water, He is percolated through the He inlet at a rate of 500 ml min^{-1} , for one hour. After this step, the He outlet is closed, and He is added until a pressure of 3 bar is reached inside the tank. For irrigation, the water outlet is opened, and a small tube is inserted through a septum into the mesocosm transparent lid for irrigation purposes.

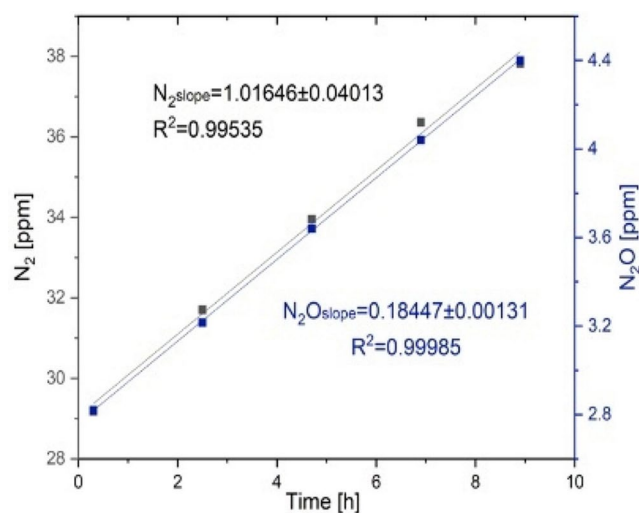


Fig. 3 Exemplary evolution of the N_2 (gray plot) and N_2O (blue plot) concentrations in the headspace of the mesocosms during one set of sampling sequences (5 sampling points per vessel)

Water baths and temperature regulation

There are two water baths with three vessels in each. The water baths are thermoregulated by two recirculating coolers (FL2503, Julabo, Germany) (Fig. 2a). The temperature of the water bath ranged from 5 to 40 °C. The water baths regulate the vessels and soil temperature during the whole incubation period and also reduce N_2 diffusion into the vessels. The water levels in the baths are regulated by pumps (Fig. 2e).

Flux rate calculation

The flux rates in this study were calculated using a semi-dynamic chamber method, where the headspace of the vessels was continuously flushed at a low gas flow rate of 40 ml min^{-1} . However, N_2 (and N_2O) still accumulates in the headspace of the mesocosms over time due to the low rate of headspace gas exchange. To calculate the flux rates for N_2 (and N_2O), we monitored changes in headspace concentrations of each vessel over a period of approximately 10–11 h. The sampling process started with vessel 1 and ended with vessel 6, involving two samples taken from each vessel at intervals of 6 min per sampling point to ensure the accuracy and consistency of the measurements. After sampling all six vessels, three injections of calibration gas were added to the GC systems. The flux rate calculations were based on sets of 5 consecutive sampling sequences (Fig. 3). For flux calculations we first corrected measured N (N_2 -N or N_2O -N) concentration values by considering the dilution effect due to the applied low rates of continuous headspace flushing (Eq. 1):

$$(1) C_{corr} = C_{sampled} + \left(C_{sampled} - C_{N_{flush}} \right) \times flowrate_{HS} \times \Delta t \times \frac{V_{HS} \times 60}{1000}$$

where the C_{corr} is the N concentration which was corrected for dilution, in ppmv, $C_{sampled}$ is the measured concentration, i.e., without correction, in ppmv, $C_{N_{flush}}$ is the concentration of N in the headspace flushing gas (i.e., a mixture of He based calibration gas and O_2 , or 0 when only He: O_2) in ppmv, $flowrate_{HS}$ is the gas mixture flow rate through the vessel headspace in ml min^{-1} , Δt is the time difference between two sampling points in hours, V_{HS} is the volume of the vessels headspace in l and 60 and 1000 are correcting factors for the units.

In all experiments, concentrations of N_2 (as well as N_2O) showed a linear increase over time. To calculate the fluxes, we used linear regression analysis (see Fig. 3). The slopes of the linear regression in ppmv N_2 or N_2O per hour were used as the basis for flux calculation.

However, for final flux calculations also the system inherent leakage rate (ILR), i.e., the rate of N₂ diffusing into the gastightly closed vessels from outside, needs to be considered. The ILR was measured repeatedly (before and after soil incubation experiments) on basis of observations of N₂ increases in empty vessels over time. The final formula used for flux calculation is given in Eq. 2:

$$(2) \text{N flux } (\mu\text{gNm}^{-2}\text{h}^{-1}) = (\text{slope} - \text{ILR}) \times \frac{V_{\text{hs}}}{V_{\text{ig}}} \times \left(\frac{mw}{T+273.15} \right) \left/ \left(\frac{A_{\text{ss}}/10,000}{P_{\text{amb}}/P_{\text{atm}}} \right) \right.$$

where the *slope*, is the (N₂ or N₂O) in ppm h⁻¹, *ILR* refers to inherent leakage rate in ppm h⁻¹ (described in the next chapter), *V_{hs}* is the volume of the headspace in the vessel in l, *V_{ig}* is the ideal gas molar volume (22.4 l mol⁻¹), *mw* is the molar mass of N₂-N, N₂O-N in g N mol⁻¹, *T* is the temperature in the vessel in °C, which with the addition of 273.15 is transformed to °K, *A_{ss}* is the soil surface area in the vessel in cm², *P_{amb}* is the air pressure in the vessel in mbar

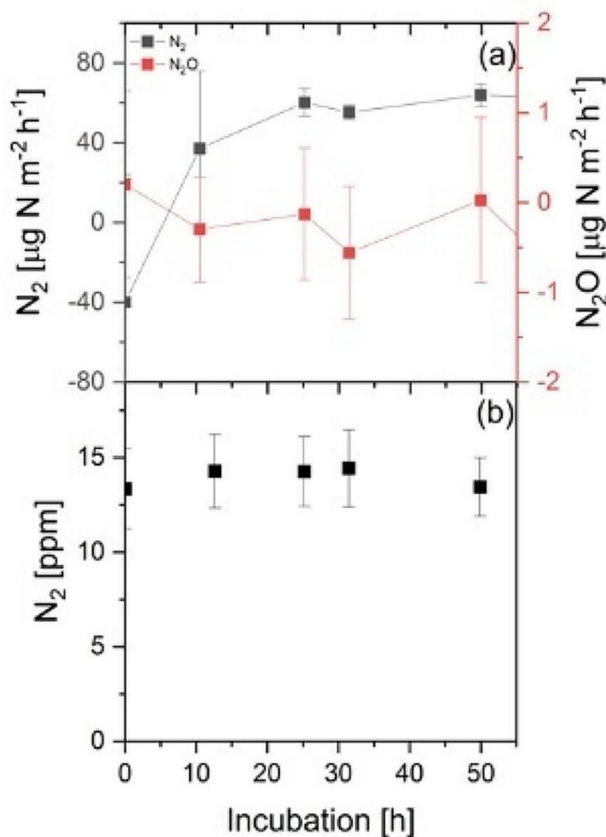


Fig. 4 Results of measurements of diffusive N₂ and N₂O fluxes into empty mesocosms vessels, which were used to determine the system ILR. Given are means of 6 vessels ± SD. (a) the black square symbols refer to N₂ fluxes, while the red square symbols refer to N₂O fluxes. (b) Change in N₂ concentrations in empty vessels with time. Given are means of 6 vessels ± SD.

and *P_{atm}* is the atmospheric air pressure in mbar. 10,000 is a unit correcting factor, which converts the final result into μgNm⁻²h⁻¹. The same flux calculation process was used for calculating CO₂-C fluxes too.

System performance

Friedl et al. (2020) provide a list of quality criteria, to be reported in denitrification studies, using the He/O₂ soil core approach, which we use in the following to assess the system performance.

Sensitivity

To determine the sensitivity or minimum detectable fluxes, we conducted empty vessel measurements, also known as the ILR measurements.

Six empty vessels were placed in water baths, and the gas exchange procedure was initiated following the aforementioned protocol. In other words, the empty vessels were alternately flushed with a predefined He/O₂ gas mixture for 10 min per hour for a total of 48 h. After the 48-hour period, the system was switched to headspace flushing using a flow rate of 40 ml min⁻¹ of a Calibration gas/O₂ mixture (Calibration gas contains 15 ppm N₂, 0.5 ppm N₂O, 500 ppm CO₂, and He (Air Liquide Germany), and the sampling sequence began. The measured N₂ fluxes, which were attributed to the diffusion of N₂ into the measuring vessel and gas lines, stabilized after approximately 12 h for all six vessels at 55 ± 10 μg N m⁻² h⁻¹ (Fig. 4a). The N₂ concentrations in the empty vessels remained at 13.9 ± 0.5 ppm N₂ (Fig. 4b), which is slightly higher than the N₂ concentration in the flushing gas mixture (12 ppm). Regarding N₂O, no diffusive fluxes into the measuring system were detectable, and therefore the ILR was set to zero (Fig. 4b).

Precision of N₂ concentration measurements

To assess the reproducibility of N₂ concentration measurements in our He soil core system, we conducted tests by flushing the system with various N₂ concentrations ranging from 1.5 to 30 ppm, while varying the background O₂ concentrations from 0 to 30% (Fig. 5). The results demonstrated excellent reproducibility of N₂ concentration measurements across the entire tested range, with a standard deviation for N₂ concentration ranging from 0.0004 to 0.08 ppm within the concentration range. The coefficient of determination (R²) for these tests was 0.9907, indicating a high level of linearity in N₂ concentration measurements.

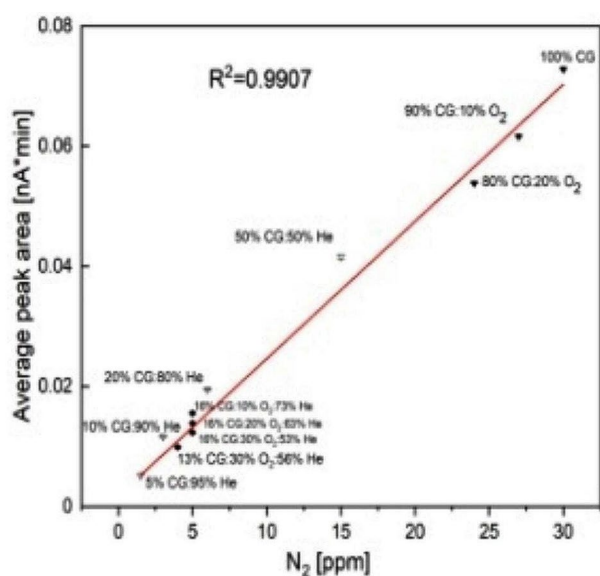


Fig. 5 Average N_2 peak area as a function of variable He/O₂ and N_2 background concentrations. The points represent mean values \pm SD, based on the average of 18 measurements per value. For each point, the exact gas composition is mentioned (CG-calibration gas)

Plant incubation experiment

To test the capabilities of the new system, we performed an incubation experiment with soil and plants. In addition to directly measuring N_2O and N_2 gas fluxes, we applied ^{15}N enriched mineral fertilizer to the soil. This allowed us to measure ^{15}N signals in both plant biomass and the soil, enabling us to establish a full ^{15}N balance. By comparing the results of the ^{15}N balance with the directly measured gaseous N_2O and N_2 losses, we could validate the accuracy and reliability of our measurements.

For this experiment, soil from abandoned cropland at CEREEP research station (Centre de Recherche en Ecologie Prédictive in Saint-Pierre-les-Nemours, France, N 48°17'14.48", E 2°40'34.64") was collected. This soil is poor cambisol (FAO 2006). The texture is sandy loam (6.9% clay, 19.0% silt, 74.1% sand). Total organic C content in this soil is 14.7 g kg⁻¹, total N is 1.19 g kg⁻¹; pH: 5.22; bulk density: 1.3 g cm⁻³ (Agapit et al. 2018). The soil was air-dried sieved to a particle size of 10 mm, and stored at the Institute for Meteorology and Climate Research (IMK-IFU) in Garmisch-Partenkirchen, Germany before being used in the experiment. 25.0 \pm 0.2 kg of dry soil was placed in layers of 0.02–0.05 m in each vessel and each layer was manually compacted to about 1.3 g cm⁻³. Prior to the start of the experiment, the soil in each vessel was fertilized with 10.3 g N m⁻² of double-labeled N fertilizer ($^{15}NH_4^{15}NO_3$; 80 atom% ^{15}N enrichment), which was applied as a solid powder and incorporated into the top 5 cm of the soil in order to simulate near-surface application. Three of the vessels

were then sown with 50 wheat seeds (*Triticum aestivum*; Saatzucht Bardowick, Germany) per vessel. The remaining three vessels served as control treatments without plants. The vessels were subjected to a 12-hour light cycle provided by light sources with an intensity of 550–630 $\mu\text{mol m}^{-2}\text{s}^{-1}$ on the soil surface and 1000–1300 $\mu\text{mol m}^{-2}\text{s}^{-1}$ at the top of the vessel when it was submerged in a water bath (the water level was 3 cm above the top of the vessel lid).

Following soil preparation, the vessels were sealed and submerged in a water bath to maintain 10 °C temperature in the soil. The vessels were then purged for 48 h with a mixture of He (5.0; purity 99.999% (Air Liquide Alphagaz, Germany) and O₂ (purity 99.998% (Air Liquide Alphagaz, Germany), with a ratio of 80:20, at a flow rate of 500 ml min⁻¹ for establishing an N₂ free atmosphere. After 48 h, the system was switched to headspace flushing mode and the flux measurements were initiated. The headspace flushing was conducted with the same gas mixture, at a flow rate of 40 ml min⁻¹. After about 3 days, the measured N_2 (and N_2O) fluxes from the air-dried soil were constant and at about 200 $\mu\text{g N m}^{-2} \text{h}^{-1}$ for N_2 and about 2.5 $\mu\text{g N m}^{-2} \text{h}^{-1}$ for N_2O , i.e., about 4 times higher as the ILR for N_2 , indicating that still N_2 residing in soil pores continued to diffuse out of the soil. As the fluxes remained low and stable, the temperature was increased to maintain 20 °C in the soil. On the subsequent incubation day, the soils were irrigated with a total of 1.6 l of water per vessel, which is equivalent to a rainfall amount of 26 mm. The irrigation process was carried out in two distinct events. This approach aimed to ensure proper water distribution and avoid excessive moisture accumulation in the lower section of the vessel. Total water addition increased the soil moisture content to approximately 20% VWC (Fig. 6).

The germination of wheat seeds began on the 6th day after sowing (two days after the irrigation). On the 25th day, an additional water application equivalent to 13 mm of rainfall was provided. Following this, on the 28th day, the temperature was raised to 25 °C to study the effects of these modifications on denitrification rates as the plants continued to grow. After a total of 33 days, the vessels were opened, and samples of both biomass and soil were collected for the analysis of total N content and the isotopic composition of ^{15}N in the plant and soil compartments.

Soil analyses

Soil samples were taken before and at the end of the experiment from each vessel for analyses of N content and enrichment in the soil. Before the incubation, the soil was sampled without separation into layers, as the soil was homogeneously mixed and dry. At the end of the experiment, three

replicated soil samples were taken from three distinct soil layers (0–10 cm, 10–20 cm, and 20–30 cm).

For the analyses, 60 g of soil was extracted with 120 ml of 2 M KCl, shaken for 60 min and filtered through Whatman filter paper. Extracts were filtered using a 0.45 µm syringe filter (Schleicher and Schuell, Dassel, Germany) and immediately frozen until analyses. Measurements of soil nitrate-N ($NO_3^- - N$) and ammonium-N ($NH_4^+ - N$) concentrations were performed colorimetrically with a microplate spectrometer (BioTek Instruments, Inc. USA), following the protocol outlined by Kempers and Zweers (1986) and Pai et al. (2021). For the validation of the volumetric water content (VWC% analysis, the soil samples were weighed and placed in 105 °C oven for 24 h.

¹⁵N fertilizer mass balance

The ¹⁵N fertilizer mass balance approach was based on a calculation of ¹⁵N excess recovery in the plant and soil N pools. The ¹⁵N enrichment of the soil N pool was determined in three soil depths. In addition, we also measured plant aboveground (AGB) and belowground biomass (BGB) and the plant N content and its ¹⁵N signal. For this, the entire AGB was collected, weighed, and oven dried at 60 °C until constant weight. By sieving and washing (3 mm mesh size), the BGB was extracted from the bulk soil, then dried at 60 °C until constant weight. AGB and BGB subsamples were blended separately into a fine powder using a ball mill (Retsch Schwingmühle MM2, Haan, Germany), then packed in tin capsules and kept in a desiccator with silica gel until the analyses. The ¹⁵N enrichment of the soil samples was determined using elemental analysis coupled to isotope ratio mass spectrometry in IMK-IFU (FlashEA, Thermo Scientific, Waltham, MA, USA). Due to technical equipment failure within our institute, the analysis of plant biomass samples was outsourced to an external laboratory (Agroislab GmbH, Germany). However, regrettably, during the analysis process, it was discovered that the level of enrichment in the samples was unexpectedly high, leading to the destruction of the BGB samples. Consequently, the limited remaining BGB material did not provide an adequate quantity for conducting further analysis or subsequent investigations.

The excess amount of ¹⁵N (mg) in all investigated pools was calculated using Eq. 3 (Zistl-Schlingmann et al. 2020):

$$(3) \text{ Excess}^{15}\text{N} = N_{\text{pool}} \times \left(\frac{\text{APE}}{100} \right)$$

where N_{pool} is the amount of N in mg found in different pools (soil, AGB, BGB) and APE (atomic percent excess) is the ¹⁵N excess enrichment of the respective pool. APE is

calculated by subtracting the natural abundance atom% ¹⁵N (we used 0.3667%) from the measured atom% ¹⁵N of the corresponding pool. Dividing the ¹⁵N excess amount by ¹⁵N addition with the fertilizer (525 mg ¹⁵N excess per mesocosm or 8.2 g ¹⁵N m⁻²) provides the ¹⁵N recovery, which is expressed in percentage.

The unrecovered ¹⁵N was assumed to be lost in gaseous form, predominantly in form of N₂. Unrecovered ¹⁵N excess is calculated by subtracting all the pools with recovered N (total soil recovery (R_{soil}) and total biomass recovery (R_{bm})). Unrecovered ¹⁵N excess multiplied by fertilizer N addition (10.3 g N m⁻²) reveals the total gaseous N loss based on ¹⁵N mass balance considerations (Eqs. 4, 5):

$$(4) \text{ UnrecoveredN} (\%) = 100 - R_{\text{bm}} - R_{\text{soil}}$$

$$(5) N_{\text{gaseouslosses}} = \text{UnrecoveredN} (\%) \times N_{\text{fertilizeraddition}}$$

Statistics

The N₂, N₂O and CO₂ fluxes during the incubation period were not normally distributed, thus in order to compare the mean fluxes of two independent groups (sown soil and bare soil vessels), the non-parametric Mann-Whitney U test was used (OriginLab 9.75 software, Northampton, USA). Differences were considered significant at $p < 0.05$.

To determine the cumulative fluxes of N₂, N₂O and CO₂, the cumulative flux for each vessel was calculated. The mean cumulative fluxes for 3 sown and 3 bare soil vessels were calculated by taking the average of the values for each treatment. The total N₂ and N₂O emissions across the entire observation period were calculated by linear interpolation between sampling points.

Results

Dynamics of measured N₂ and N₂O emissions in planted and bare soils

The time course of N₂O, N₂ and CO₂ gas fluxes is presented in Fig. 6. After the initial 48-hour period of gas exchange, followed by an additional 24-hour period where flux measurements gradually decreased, N₂ fluxes reached a stable value of approximately 0.25 mg N m⁻² h⁻¹. Similarly, N₂O fluxes stabilized at around 2.5 µg N m⁻² h⁻¹ during this period. Soil respiration rates were as low as 2.5 mg C m⁻² h⁻¹, indicating low microbial activity in the air-dried soil. Following the temperature increase to 20 °C, the N emissions slightly increased to 0.26 mg N m⁻² h⁻¹ and 4 µg N m⁻² h⁻¹, for N₂ and N₂O, respectively, and to 7 mg C

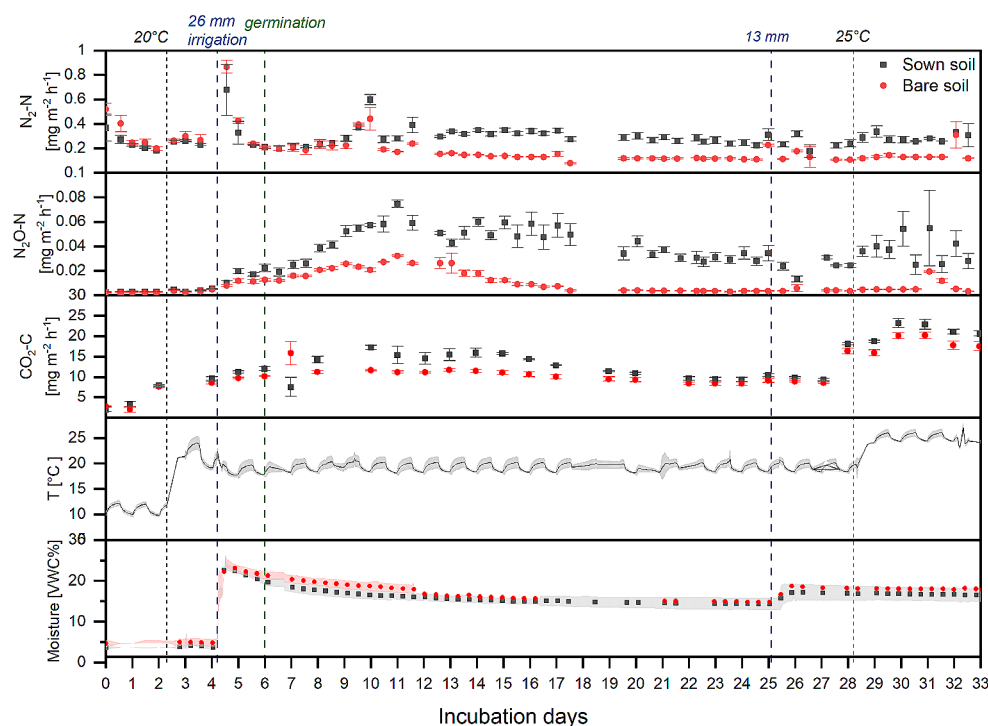
$\text{m}^{-2} \text{h}^{-1}$ for soil respiration. The following soil irrigation triggered an increase in N_2 fluxes, with values reaching up to $6.3 \text{ mg N m}^{-2} \text{ h}^{-1}$ ($1.5 \text{ kg N ha}^{-1} \text{ day}^{-1}$), while N_2O fluxes increased up to $20 \mu\text{g N m}^{-2} \text{ h}^{-1}$ ($0.005 \text{ kg N ha}^{-1} \text{ day}^{-1}$), though no distinct peak was observed as for N_2 fluxes. Instead, N_2O fluxes gradually increased over time and showed the highest values 5 days after the germination. CO_2 fluxes also did not peak after the irrigation, but gradually increased 4 days after the germination.

Plant germination and growth became visible on day 6 of the experiment. From that point onwards, the AGB exhibited a height and biomass increase, with an average daily growth rate ranging between 2 and 3 cm (as was visually estimated). However, once the plants reached the top of the vessel, it was no longer possible to estimate their growth rate visually. N_2 fluxes remained relatively stable during the plant growth period. With increasing plant biomass development, a significant difference ($p < 0.001$) in N_2 fluxes between the sown and bare soil vessels became apparent. N_2 (days 6–25) in sown soil were $0.29 \pm 0.01 \text{ mg N m}^{-2} \text{ h}^{-1}$ and $0.17 \pm 0.01 \text{ mg N m}^{-2} \text{ h}^{-1}$ in bare soil (0.071 ± 0.003 and $0.040 \pm 0.003 \text{ kg N ha}^{-1} \text{ day}^{-1}$, respectively). N_2O fluxes reached maximum values at day 11, both in sown and bare soil vessels, resulting in 0.075 ± 0.003 and $0.032 \pm 0.001 \text{ mg N m}^{-2} \text{ h}^{-1}$ respectively (0.0179 ± 0.0007 and $0.0077 \pm 0.0001 \text{ kg N ha}^{-1} \text{ day}^{-1}$). After reaching their peak values, the emissions of N_2O in the bare soil decreased within a few days and returned to almost the same values as before the irrigation, which were around $3\text{--}4 \mu\text{g N m}^{-2} \text{ h}^{-1}$. The mean fluxes of N_2O during the plant growth

period (days 6–25) were $0.043 \pm 0.002 \text{ mg N m}^{-2} \text{ h}^{-1}$ and $0.013 \pm 0.002 \text{ mg N m}^{-2} \text{ h}^{-1}$, in sown and bare soil, respectively (0.010 ± 0.001 and $0.0031 \pm 0.0004 \text{ kg N ha}^{-1} \text{ day}^{-1}$). In sown vessels, the N_2O fluxes remained high for a longer period and only decreased to a minimum value of $0.013 \text{ mg N m}^{-2} \text{ h}^{-1}$ on day 26. The additional irrigation (day 25) and increase in temperature (day 28) did not contribute to increase in fluxes, resulting in a slight decrease in N fluxes. Mean N_2 fluxes were $0.27 \pm 0.01 \text{ mg N m}^{-2} \text{ h}^{-1}$ and $0.14 \pm 0.01 \text{ mg N m}^{-2} \text{ h}^{-1}$ in sown and bare soil, respectively. N_2O mean fluxes after the second irrigation were $0.033 \pm 0.003 \text{ mg N m}^{-2} \text{ h}^{-1}$ and $0.006 \pm 0.001 \text{ mg N m}^{-2} \text{ h}^{-1}$, in sown and bare soil, respectively. The mean N_2O mole fraction, defined as $\text{N}_2\text{O}/(\text{N}_2\text{O} + \text{N}_2)$, during the plant growth period was 0.121 ± 0.004 in sown vessels and 0.059 ± 0.005 in bare soil vessels.

Following germination, photosynthesis became a significant contributor to CO_2 uptake. As plant biomass increased, headspace CO_2 concentrations dropped from about 500–700 ppmv during the dark period to about 250–300 ppmv when the lights were turned on within 5 min and stayed at that level during the entire light period. This hampered our ability to determine CO_2 flux rates during daytime. Therefore, the CO_2 flux rates shown in Fig. 6 represent only the rates of night-time soil and AGB respiration. The soil respiration rates slightly increased in sown soil vessels with plant biomass development ($12.9 \pm 0.8 \text{ mg N m}^{-2} \text{ h}^{-1}$ and $10.6 \pm 0.5 \text{ mg N m}^{-2} \text{ h}^{-1}$ in sown and bare soil respectively, from plants germination until the second irrigation at day 25). The second irrigation event exhibited no discernible impact

Fig. 6 The time course of N_2 , N_2O and CO_2 fluxes across the entire experimental period. The black symbols refer to N and C gas fluxes from sown soils, while the red symbols refer to gas fluxes measured from bare soil. Given are means \pm SE of three replicates (three mesocosms per treatment). Black line plot represents the mean soil temperatures in the upper layer of the 6 vessels \pm SE. Moisture plot represents the VWC% in the upper soil layer of the sown and bare soil vessels \pm SD.



on nocturnal fluxes. However, the subsequent increase in soil temperature from 20 to 25 °C significantly stimulated flux rates in both sown and bare vessels ($20.8 \pm 0.8 \text{ mg N m}^{-2} \text{ h}^{-1}$ and $17.9 \pm 0.7 \text{ mg N m}^{-2} \text{ h}^{-1}$, respectively).

Statistical analysis was conducted to reveal the effect of the growing plants on the denitrification rates, thus the incubation period was analyzed separately at each stage (dry rewetting, germination, additional rewetting and temperature increase). Significant differences (higher N fluxes in sown soil vessels) were found in N and C fluxes (soil and AGB respiration rates), between sown and bare soil vessels. The differences in N fluxes were significant ($P < 0.001$) only for the period following germination and plant biomass development, indicating a direct effect of plant growth on N gas fluxes (Table 1). Also, for soil and AGB respiration rates, i.e., the sum of heterotrophic and autotrophic respiration statistically higher nighttime fluxes were observed for sown vessels.

The cumulative fluxes of N_2 over the entire experimental period were $316 \pm 8 \text{ mg N m}^{-2}$ and $225 \pm 12 \text{ mg N m}^{-2}$, respectively (Fig. 7). N_2O cumulative fluxes were $28 \pm 2 \text{ mg N m}^{-2}$ in sown soil, and $7.6 \pm 0.3 \text{ mg N m}^{-2}$ in bare soil vessels. Carbon dioxide cumulative respiration fluxes in sown soil vessels were 4.8 ± 0.1 and $4.0 \pm 0.1 \text{ g C m}^{-2}$ respectively in bare soil vessels. The total cumulative N gas losses ($\text{N}_2 + \text{N}_2\text{O}$) were $344 \pm 7 \text{ mg N m}^{-2}$ and $232 \pm 10 \text{ mg N m}^{-2}$, in sown soil and bare soil respectively (Table 2).

Comparison of measured N_2 and N_2O emissions with results from the ^{15}N mass balance approach

To verify the accuracy of the measured gaseous N losses in the form of N_2 and N_2O , we additionally conducted a ^{15}N mass balance of the applied fertilizer (10.3 g N m^{-2}). The total recovery rate of ^{15}N in sown mesocosms was $84 \pm 5\%$, while in the bare soil mesocosms, the recovery was $84 \pm 6\%$ (Table 2). Total fertilizer N recovery was $8.6 \pm 0.5 \text{ g N m}^{-2}$ and $8.7 \pm 0.6 \text{ g N m}^{-2}$ in sown and bare soil vessels, respectively. In planted as well as in bare mesocosms $> 48\%$ of recovered ^{15}N was found in the 0–10 cm soil layer. In the sown vessels, the ^{15}N recovery in the AGB was determined to be $8.1 \pm 0.9\%$. However, measurements of the BGB are not available due to the loss of samples. However, considering that the total amount of BGB in the sown vessels was estimated to be $0.8 \pm 0.1 \text{ g}$, and considering the previously measured enrichment of the same wheat species in the same system, it can be approximately assumed that the recovery in the BGB was about 0.4%. Thus, it can be concluded that the recovery in BGB would be almost negligible.

The unrecovered ^{15}N , which was interpreted as gaseous losses (as our mesocosms don't allow for leaching), amounted to $1.7 \pm 0.5 \text{ g N m}^{-2}$ ($16.5 \pm 4.9\%$) and $1.6 \pm 0.6 \text{ g}$

Table 1 The mean N_2 and N_2O fluxes ($n=3$) (in $\text{mg N m}^{-2} \text{ h}^{-1}$) and cumulative (in mg N m^{-2}) for different periods of the incubation experiment. The *** symbol indicates statistical significance at $p < 0.001$ between the means of two treatments. Blue vertical lines highlight periods of rewetting and temperature elevation, whereas the green line marks the point of germination

Treatment	Dry soil (days 0-2.5 [temperature (T) = 10 °C])		Temperature increase and rewetting (days 2.5-6) [temperature (T) = 20 °C]		Plants growth (days 6-25) [T = 20 °C]		T increase and rewetting (days 25-33) [T = 25 °C]		Total incubation period (days 0-33)	
	N_2	N_2O	N_2	N_2O	N_2	N_2O	N_2	N_2O	N_2	N_2O
Sown soil	Mean	0.22 ± 0.02	0.034 ± 0.003	1.1 ± 0.8	0.0108 ± 0.003	0.29 ± 0.01***	0.27 ± 0.01***	0.033 ± 0.002***	0.33 ± 0.002***	0.45 ± 0.05***
	Cumulative	15 ± 2	0.17 ± 0.01	114 ± 10	0.8 ± 0.1	134 ± 1	55 ± 4	6.9 ± 1.1	316 ± 8	28 ± 2
Bare soil	Mean	0.27 ± 0.01	0.029 ± 0.002	1.0 ± 0.7	0.007 ± 0.001	0.17 ± 0.01	0.14 ± 0.01	0.006 ± 0.001	0.010 ± 0.001	0.12 ± 0.01
	Cumulative	20 ± 1	0.14 ± 0.01	103 ± 9	0.53 ± 0.05	73 ± 4	30 ± 3	1.2 ± 0.1	225 ± 12	7.6 ± 0.3

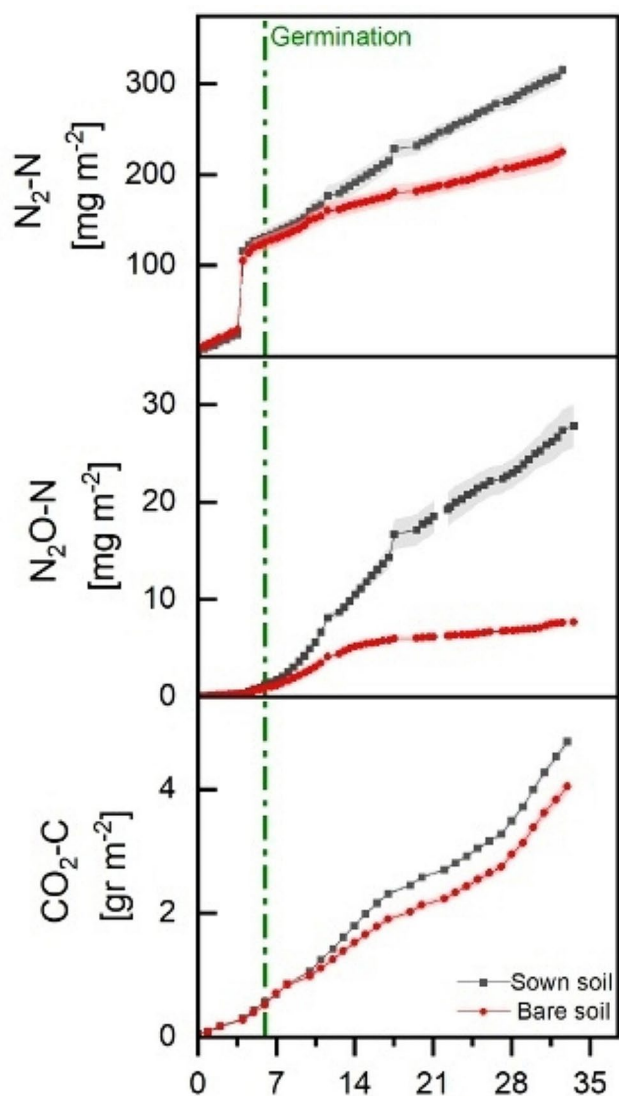


Fig. 7 Cumulative N fluxes in mg m^{-2} for $\text{N}_2\text{-N}$ and $\text{N}_2\text{O-N}$, and soil+AGB respiration rates in g m^{-2} for $\text{CO}_2\text{-C}$ over the 33-day incubation period. The grey plots represent the mean values for sown soil vessels ($n=3$), the red plots represent the mean values for bare soil vessels ($n=3$), while the green dashed line indicates the onset of germination. The shaded regions depict the standard error

N m^{-2} ($15.5 \pm 5.8\%$) in sown and bare mesocosms, respectively. These findings indicate higher N losses than those estimated through the direct measurements of N_2 and N_2O fluxes. However, given the overall relatively low denitrification fluxes and relatively low precision of the ^{15}N mass balance approach, a conclusive comparison between both methods was not possible.

Discussion

In this study, we used a newly developed system to measure gaseous N losses from planted soil under controlled light conditions. This system stands out because it facilitates the growth of plants from seeding to harvest over long periods (from weeks to months). This capability provides a unique opportunity to explore the impact of plant development on denitrification processes.

The system performance

One of the most important factors in this type of soil mesocosm system is the sensitivity with which N fluxes can be measured. To ensure the accuracy and reliability of our measurements, we conducted tests to assess the reproducibility of N_2 concentrations using different gas mixtures. The results of these tests showed that the detector used in our system exhibited high linearity over a wide range of N_2 concentrations (Fig. 5). Importantly, the measured N_2 concentrations were not affected by variations in the mixtures of He and O_2 used in the experiments.

As a second step we evaluated the system inherent leakage rate (ILR), which describes the diffusive influx of N_2 from the outside into the mesocosm and gas sampling system. This is a major challenge as ambient N_2 concentrations are around 80% so that even tiny leaks or leaky seals can result in large influxes of N_2 from the outside into the system (Butterbach-Bahl et al. 2002). In our experiments with empty mesocosms an influx of N_2 of $55 \pm 10 \mu\text{g N m}^{-2}\text{h}^{-1}$ ($13 \text{ g N ha}^{-1} \text{ day}^{-1}$) was measured, while an influx of N_2O was not detectable. Another problem is N_2 scavenging in soil pores and materials used for the system construction. However, this problem can be limited by long flushing periods with He/ O_2 gas mixtures (Burgin et al. 2010; Butterbach-Bahl et al. 2002; Wang et al. 2011) and was not relevant for our measurements, as the measuring periods were always well over 20 days, while in previous experiments, soil incubations were usually completed after 2–3 days (e.g., Dannenmann et al. 2008; Wang et al. 2011, 2020).

In our experimental setup, we utilized vessels with a volume of 37 l, of which the headspace accounted for 16 l of the total volume. In addition, the soil surface area within the vessels was measured to be 0.064 m^2 . It is worth noting that our system had a significantly larger capacity than other systems described. Furthermore, to the best of our knowledge, our setup is one of the few that allows for the growth of plants under these experimental conditions. For example, Wang et al. (2011) achieved a detection limit of $8.1 \mu\text{g N}_2\text{-N m}^2 \text{ h}^{-1}$ with a total vessel volume of about 1.8 l. The detection limit achieved by Wang et al. (2011) was an improvement of about 20% as compared to the

Table 2 Applied N (10.3 g N m⁻²) total recovery in soil and plant biomass and gaseous N losses. The table summarizes cumulative N emissions (N₂ and N₂O) across the entire experimental observation period (33 days) as well as calculated recovery rates for applied ¹⁵NH₄¹⁵NO₃-N and total applied N in above-ground plant biomass and soil sown soil (S1, S2, S3) and bare soil (B1, B2, B3). The unrecovered N is assumed to represent gaseous N losses. The means error is SE of three replicates for each treatment (3 vessels). The abbreviation “ds” refers to “dry soil”

Vessel	Soil depth [cm]	N ₂ [mg N m ⁻²]	N ₂ O [mg N m ⁻²]	N ₂ +N ₂ O [mg N m ⁻²]	Soil weight [kg ds]	Total N [mg N kg ⁻¹ ds]	Soil ¹⁵ N atom%	Plant dry weight vessel ⁻¹ [g]	Plant bio-mass ¹⁵ N atom%	Total N Recovery [g N m ⁻²] (%)	Unrecovered N [g N m ⁻²] (%)		
S1	0–10				10.1	500	6.11			5.7 (55.4)			
	10–20				6.9	500	1.55			0.8 (7.8)			
	20–30				7.7	400	0.85			0.3 (2.9)			
	AGB							3.17	31.00	0.9 (9.6)			
	BGB							0.99	n/a	n/a			
	N-gas	331.4	25.9	357.3	Ratio (N ₂ O/(N ₂ O+N ₂))=0.07							0.08±0.01	
	Total									7.7 (74.7)	2.6 (25.2)		
S2	0–10				9.7	600	6.03			6.5 (63.0)			
	10–20				7.2	600	1.49			0.9 (9.3)			
	20–30				8.3	600	1.00			0.6 (6.0)			
	AGB							3.44	39.9	0.9 (9.6)			
	BGB							0.64	n/a	n/a			
	N-gas	308.1	32.3	340.4	Ratio (N ₂ O/(N ₂ O+N ₂))=0.09								
	Total									6.1 (59.2)			
S3	0–10				9.1	600	6.04			1.8 (17.5)			
	10–20				8.5	600	2.16			0.7 (6.8)			
	20–30				8.3	600	1.05			0.7 (6.8)			
	AGB							3.30	33.43	0.7 (6.8)			
	BGB							0.82	n/a	n/a			
	N-gas	307.9	25.3	333.2	Ratio (N ₂ O/(N ₂ O+N ₂))=0.08								
	Total									9.3 (90.3)	1.0 (9.7)		
Mean	N-gas	316±8 (3.06)	28±2 (0.27)	344±7 (3.3)	Ratio (N ₂ O/(N ₂ O+N ₂))=0.08±0.01								
sown (n=3)	0–10				9.6±0.3	567±33	6.06±0.03			6.1±0.2 (59.2)			
	10–20				7.5±0.5	567±33	1.7±0.2			1.2±0.3 (11.3)			
	20–30				8.1±0.2	533±67	1.0±0.1			0.5±0.1 (5.2)			
	AGB							3.30±0.08	34.8±2.7	0.8±0.1 (8.1)			
	BGB							0.8±0.1	n/a				
	Total									8.6±0.5 (83.8)	1.7±0.5 (16.5)		
	B1	0–10				7.6	500	6.25			4.9 (48.0)		
10–20					8.2	500	1.81			1.2 (11.7)			
20–30					9.5	600	1.52			1.3 (12.6)			
N-gas		245.7	7.2	252.9	Ratio (N ₂ O/(N ₂ O+N ₂))=0.03								
Total										7.4 (71.8)	3.0 (29.5)		
B2		0–10				8.5	600	6.92			7.3 (70.9)		
		10–20				8.4	600	1.75			1.4 (13.6)		
	20–30				8.0	600	1.05			0.65 (6.3)			
	N-gas	203.0	7.5	210.5	Ratio (N ₂ O/(N ₂ O+N ₂))=0.04								
	Total									9.3 (90.3)	1.0 (9.7)		
	B3	0–10				7.8	600	5.64			5.4 (52.4)		
		10–20				6.3	600	4.08			2.8 (27.2)		
20–30					10.4	600	1.21			1.0 (9.7)			
N-gas		225.7	8.2	233.9	Ratio (N ₂ O/(N ₂ O+N ₂))=0.04								
Total										9.2 (89.9)	1.1 (10.7)		
Mean		N-gas	225±12 (2.18)	7.6±0.3 (0.07)	232±10 (2.2)	Ratio (N ₂ O/(N ₂ O+N ₂))=0.04±0.00							
bare (n=3)		0–10				7.8±0.3	550±33	3.7±0.4			5.9±0.7 (57.0)		
	10–20				8.2±0.7	500±33	1.8±0.8			1.8±0.5 (17.5)			
	20–30				9.5±0.7	600±0	1.5±0.1			1.0±0.2 (9.5)			
	Total									8.7±0.6 (84.0)	1.6±0.6 (15.5)		

system developed by Butterbach-Bahl et al. (2002) and a 4-fold improvement of the performance by Cárdenas et al. (2003) for a gas-flow-soil-core system. To our knowledge, the only system that allows plant growth and is based on the He/O₂ soil-core-method was developed by Senbayram et al. (2020). The detection limit of this system for N₂ was reported to be $\geq 10 \text{ g N ha}^{-1} \text{ day}^{-1}$, which is comparable to the sensitivity of the system discussed in our study. However, the volume of the system by Senbayram et al. (2020) was approximately 16 times smaller than our system.

Soil N₂ and N₂O fluxes and plant effects

In our experiment, N₂+N₂O fluxes were relatively modest, representing 2.2–3.3% of the applied fertilizer N over a period of 33 days. It is well known that soil moisture is one of the most important factors controlling denitrification (Butterbach-Bahl et al. 2002; Friedl et al. 2016), as O₂ diffusion into the soil matrix is hindered at elevated soil moisture levels. Under such conditions, denitrification is enhanced because denitrifying microorganisms use NO₃⁻ as an alternative electron acceptor (Knowles 1981). The soil used in our experiment had a sandy texture with low water holding capacity ($37 \pm 2\%$ WHC, data not shown). Therefore, we assume that the applied irrigation rates were too low to promote anaerobic conditions in the soil, so that denitrifying conditions only prevailed for a short time immediately after the irrigation events.

This interpretation is also supported by our observation that after the first irrigation event, which was also accompanied by an increase in soil temperature from 10 to 20 °C, N₂ emissions showed a distinct emission peak over a period of about 36 h, while the increase in N₂O emissions during this period was much smaller. The rapid decline in N₂ fluxes after the initial peak suggests a transient anaerobic environment triggered by the irrigation event. The initial spike in N₂ fluxes likely represents the rapid consumption of accumulated NO₃⁻ in the soil due to the sudden increase in anoxic conditions, as has also been observed in other experiments with direct N₂ and N₂O flux measurements (e.g., Wang et al. 2011, 2020). However, the subsequent rapid decrease in N₂ fluxes indicates that these anoxic conditions were short-lived.

When comparing our results for peak N₂ fluxes with results obtained in previous incubation studies using the He gas flow soil core technique (Cárdenas et al. 2003; Senbayram et al. 2020; Wang et al. 2011), it becomes clear that the fluxes observed in our study are rather low. E.g., Senbayram et al. (2020) using a system similar to ours reported, peak N₂ fluxes as high as approximately $1 \text{ mg N m}^{-2} \text{ h}^{-1}$ in sown soil amended with KNO₃, i.e., about twice as high as in our study. Moreover, N₂O peaks in the Senbayram et

al. (2020) study were approximately $591 \pm 279 \text{ } \mu\text{g N m}^{-2} \text{ h}^{-1}$, thus one magnitude higher than in our experiment. Moreover, the ratio of (N₂O)/(N₂O+N₂) in our study with a soil column depth of about 0.3 m were in the range of 0.03–0.09, which is about one order of magnitude lower than in the study of Senbayram et al. (2020) (range: 0.33–0.73, soil height about 0.05–0.10 m). This suggests, that soil column height, and thus the diffusion length of N₂O in the soil matrix from its point of production towards the soil-atmosphere interface, is likely to shift the (N₂O)/(N₂O+N₂) ratio towards N₂ due to the consumption of N₂O by denitrification during its passage through the soil matrix (Butterbach-Bahl et al. 2013; Friedl et al. 2020). Senbayram et al. (2020) argue, that nitrification was a significant contributor to N₂O production. In contrast, our study lacked the ability to discriminate between different processes. Cárdenas et al. (2003) quantified N₂ and N₂O fluxes from grassland soils amended with 50 kg N as KNO₃ ha⁻¹ and 360 kg glucose-C ha⁻¹ and found peak emissions of N₂ fluxes of $10.8 \text{ mg N m}^{-2} \text{ h}^{-1}$ and of N₂O fluxes of about $40 \text{ mg N m}^{-2} \text{ h}^{-1}$, fluxes more than 2–3 orders of magnitudes higher than in our study. However, these differences may be explained by differences in soil texture, with the soil used by Cárdenas et al. (2003) having a clay content of 37%, compared to 7% in our soil, and in the simultaneous provision of NO₃⁻ and an easily degradable carbon source, which are factors known to significantly enhance denitrification rates (Butterbach-Bahl et al. 2013; Groffman et al. 2007).

The results of our study revealed a temporal disparity between the peak fluxes of N₂O and N₂, with the peak flux of N₂O occurring after the peak flux of N₂ (Fig. 6). In contrast to the clear peak observed for N₂, the N₂O flux showed a more diffuse pattern, gradually increasing before finally decreasing. This discrepancy suggests that the dynamics of N₂O production and emission are different from those of N₂. This observation is controversial to what was shown in previous studies (Cárdenas et al. 2003; Gao et al. 2023; Meijide et al. 2010; Wang et al. 2011). In these studies, peaks of both N₂ and N₂O occur after N addition to the system, similar to our observation, while N₂O maxima occur before N₂ maxima. The reason for this remains unclear, as it is usually assumed that the denitrification chain is expressed sequentially. However, a recent report by Lycus et al. (2018) suggests that denitrifiers may follow a bet-hedging approach, i.e., the nitrous oxide reductase *nosZ*, which catalyzes the reduction of N₂O to N₂, is always expressed, while other enzymes of the denitrification chain may not be expressed. This may explain our observation, but final clarification can only be achieved by studying N₂ and N₂O flux dynamics for different soils, accompanied by analyses of denitrification gene expression and enzyme activity dynamics.

In our study, we observed that during the plant growth period, soil N_2 fluxes were 1.8 times higher and N_2O fluxes were 4 times higher compared to bare soil (Table 1). Similar results have been reported previously (Scholefield et al. 1997; Senbayram et al. 2020; Smith and Tiedje 1979; Stefanson 1972). This observation can be explained by increased microbial activity in the rhizosphere zone. The microbial activity mainly takes place in the rhizosphere due to root exudates and can alter C and N transformations in the vicinity of plant roots (Bais et al. 2006; Ma et al. 2022). In soil-grown plants, nearly half of the fixed C is partitioned to the soil, with 50% partitioned to root tissues and the remaining 50% to root products such as root exudates (Neumann et al. 1999). In cereals, about 5% of the net C fixed during photosynthesis is released into the soil and becomes available to the soil microbial community (Farrar et al. 2003). Although root exudates represent a small fraction of the total C input, they are an integral part of the global C and N cycle. However, the exact mechanism by which root exudates affect denitrification is complex and not fully understood (Coskun et al. 2017). E.g., a recent study linking root exudation of barley, wheat and ryegrass with denitrification enzyme activity not only found either stimulating or inhibiting effects of different root exudation compounds, but also showed that the same compounds can exert contradictory effects on denitrification in different soils (Maurer et al. 2021). Plant age appears to be another significant factor influencing outcomes (Von Rheinbaben and Trolldenier 1984).

Previous studies have provided insight into the potential effects of plants on denitrification. Malique et al. (2019) demonstrated higher denitrification potential in planted cropland soils, suggesting a direct effect of plants. They also observed an exponential decrease in denitrification potential with increasing shoot and root biomass, which is consistent with our findings of decreasing N_2 flux rates over the course of the incubation period (Fig. 6). Similarly, other studies have observed the direct influence of plants on denitrification through rhizosphere processes. Rummel et al. (2021) showed in their study with pre-cultivated plants, that plant and root growth, together with water and N uptake, were the main regulators of denitrification. In addition, Klemmedtsson et al. (1987) found a positive correlation between denitrification rates and root biomass, with N_2 being the dominant denitrification product near roots. In contrast, Haider et al. (1987) conducted a study where they did not observe an increase in denitrification following the growth of two-week-old corn seedlings. They concluded that the root exudates produced by the plants were not able to stimulate the denitrification process. Recent studies (Senbayram et al. 2018; Wu et al. 2018) suggest that soil NO_3^- concentration is likely to be the primary factor regulating denitrification

end products. However, in our study, this explanation is not sufficient to explain the differences in denitrification fluxes, as there was no significant difference in NO_3^- availability between the two treatments (data not shown). Taken together, these results suggest that while plants can influence denitrification, additional factors beyond root exudates may play a significant role in limiting the denitrification process.

Comparing directly measured gaseous N_2 and N_2O fluxes with results of a ^{15}N mass balance approach

Few comparisons have been made between different denitrification measurement techniques, particularly between in situ and in vitro techniques (Groffman et al. 2007; Lewicka-Szczebak et al. 2017). The ^{15}N mass balance method allows direct assessment of the fate of applied N in the field or in the laboratory, whereas the He soil core technique can only be used in the laboratory and can provide direct measurements of N_2O and N_2 fluxes in high temporal resolution. In this study, we compared directly measured, cumulative N_2 and N_2O fluxes over the entire experimental period of 33 days with the amount of unrecovered ^{15}N .

The results of the comparison indicate that the cumulative losses of N_2 and N_2O fluxes, totaling 0.23–0.34 g N m^{-2} over a 33-day incubation period, were lower than the estimates of N losses obtained by the ^{15}N mass balance approach (about 1.6–1.7 g N m^{-2}). Similar comparisons of ^{15}N mass balance with other methods for measuring denitrification (acetylene inhibition technique, ^{15}NGF method) have been performed previously (Heinemeyer et al. 1988; Mosier et al. 1986; Parkin et al. 1985). All of these studies reached the consensus that estimates of denitrification N losses were higher when based on the ^{15}N mass balance method. Our observation is consistent with the findings of Heinemeyer (1988), who reported that direct N emissions accounted for approximately 20% of the unrecovered N from the ^{15}N mass balance. In the context of ^{15}N balance measurements applied to pasture systems, previous studies (Bristow et al. 1987; Clough et al. 1998b; Whitehead and Bristow 1990) have also suggested that over 20% of the ^{15}N input may remain unaccounted for. Although most comparisons are based on in situ measurements, there are obvious limitations associated with the ^{15}N balance in He soil core systems. There are several possible reasons for this discrepancy. First, these unaccounted losses could be due to NH_3 volatilization. Although the soil in our study was slightly acidic and the fertilizer was incorporated and mixed into the topsoil, there is uncertainty in the actual amount of NH_3 that can be lost in our continuously flushed system. NH_3 volatilization is influenced by several factors, including soil pH, NH_3 partial pressure between the air and soil atmosphere,

wind speed, SOC content, soil texture, moisture content, and temperature (Bouwman et al. 2002b). The experimental system used in this study involved a sequential flushing process characterized by high flow rates initiated from the soil surface, followed by passage of the flushing mixture through the headspace. Simultaneously, the soil conditions were maintained in a wet state and the temperature was elevated. Under these specific conditions, it is plausible to anticipate an increased potential for NH_3 emissions. Moreover, such effects may be more pronounced in bare soil systems because the presence of plants has the capacity to mitigate NH_3 volatilization. It is well documented that NH_3 losses from synthetic fertilizer applications average about 12% (Ma et al. 2021). Two additional factors contributing to this discrepancy are unrecovered BGB and NO emissions. However, the contribution of roots to the total biomass recovery in our study is likely to be minimal (around 0.4%) due to their relatively low weight. Regarding NO emissions, it is important to emphasize that although NO can be emitted from both soil and plant leaves, the magnitude of its loss is not expected to be excessive (del Río et al. 2004). NO emissions are generally lower than N_2O emissions, which account for a relatively small fraction of N losses in our incubation study (Bouwman et al. 2002a). Another uncertainty associated with estimating N losses using the mass balance approach is greater due to the presence of multiple N components and their spatial variability within the experimental vessels as well as in field experiments. This leads to a higher degree of uncertainty in the mass balance calculations compared to the direct method. The direct measurement method, on the other hand, shows greater precision in quantifying total N losses by avoiding the additive error accumulation that occurs in the mass balance approach (Myrold 1990). There is also evidence that the gaseous forms of N can be trapped in the soil and released after destructive sampling. Clough et al. (1998a) found that up to 16% of the applied ^{15}N was trapped as gas ($\text{N}_2+\text{N}_2\text{O}$) in the soil pore space 38 days after ^{15}N application in the soil columns studied. Considering the wide range of factors influencing the observed discrepancies, it is evident that the ^{15}N mass balance method generally yields higher estimates compared to direct measurements, although within the average range reported in similar studies. The unrecovered ^{15}N is within the range of the average unrecovered N in other studies.

Short-comes of the measuring system

While significant progress has been made, it is important to recognize persistent technical limitations that warrant future consideration. An observed limitation during the incubation phase was the inadequacy of daytime CO_2 levels due to photosynthetic CO_2 fixation. As plant biomass increased,

headspace CO_2 concentrations dropped from about 500–700 ppmv during the dark period to about 250–300 ppmv when the lights were turned on within 5 min. To address this challenge, a recommended solution involves the implementation of dynamic CO_2 dosing in the gas mixture introduced into the vessels. This strategy holds great promise for correcting the CO_2 deficiency that occurs during daylight hours. Another unresolved challenge relates to O_2 dynamics, specifically the potential disruption of anaerobic microenvironments during soil purging to replace the initial atmosphere with an N_2 -free atmosphere. To mitigate this problem, a viable solution is to provide an adequate period of time for the re-establishment of anaerobic conditions by soil respiration. This requires careful monitoring of soil O_2 levels and inhibition of microbial activity prior to commencing measurements. Another problem is the formation of condensation water on the surface of the upper parts of the vessel. An internal air circulation system for each individual vessel, with on-line measurement of CO_2 concentration and redosing of CO_2 , as well as a unit for controlling humidity, will in the future make it possible to solve both the CO_2 and water condensation problems.

Subsequent incubations could provide valuable insights by incorporating the ^{15}NGF method (Friedl et al. 2020) to measure N fluxes in addition to existing techniques. This approach would allow differentiation between denitrification pools resulting from applied fertilizer and those resulting from the intrinsic N content of the soil.

Conclusion

The new He atmosphere incubation system presented here allows direct and highly sensitive detection of N_2 and N_2O emissions. The precision and sensitivity of the system are comparable to other similar systems, but it has significantly larger headspace and soil volumes, combined with tunable light accessibility and the potential for simultaneous CO_2 flux measurements and soil O_2 monitoring. Together, these advances make this system a distinctive and versatile tool for investigating the various factors that control denitrification, particularly the influence of plants. As a result, this system has the potential to make significant contributions to our understanding of denitrification mechanisms in terrestrial ecosystems and how plants and light availability affect denitrification in the rhizosphere.

Supplementary Information The online version contains supplementary material available at <https://doi.org/10.1007/s00374-024-01809-w>.

Funding This study was funded by the German Research Foundation (DFG) within the research unit DASIM. KBB received additional funding by the Pioneer Center for Research in Sustainable Agriculture

(Land-CRAFT), DNR Grant P2.
Open Access funding enabled and organized by Projekt DEAL.

Declarations

Competing interests The authors have no relevant financial or non-financial interests to disclose. The authors have no competing interests to declare that are relevant to the content of this article. All authors certify that they have no affiliations with or involvement in any organization or entity with any financial interest or non-financial interest in the subject matter or materials discussed in this manuscript. The authors have no financial or proprietary interests in any material discussed in this article.

Open Access This article is licensed under a Creative Commons Attribution 4.0 International License, which permits use, sharing, adaptation, distribution and reproduction in any medium or format, as long as you give appropriate credit to the original author(s) and the source, provide a link to the Creative Commons licence, and indicate if changes were made. The images or other third party material in this article are included in the article's Creative Commons licence, unless indicated otherwise in a credit line to the material. If material is not included in the article's Creative Commons licence and your intended use is not permitted by statutory regulation or exceeds the permitted use, you will need to obtain permission directly from the copyright holder. To view a copy of this licence, visit <http://creativecommons.org/licenses/by/4.0/>.

References

- Agapit C, Gigon A, Blouin M (2018) Earthworm effect on root morphology in a split root system. *Plant Biosyst* 152:780–786. <https://doi.org/10.1080/11263504.2017.1338627>
- Bais HP, Weir TL, Perry LG, Gilroy S, Vivanco JM (2006) The role of root exudates in rhizosphere interactions with plants and other organisms. *Annu Rev Plant Biol* 57:233–266. <https://doi.org/10.1146/annurev.arplant.57.032905.105159>
- Bakken LR (1988) Denitrification under different cultivated plants: effects of soil moisture tension, nitrate concentration, and photosynthetic activity. *Biol Fertil Soils* 6:271–278. <https://doi.org/10.1007/BF00261011>
- Bobbink R, Hornung M, Roelofs JGM (1998) The effects of air-borne nitrogen pollutants on species diversity in natural and semi-natural European vegetation. *J Ecol* 86:717–738. <https://doi.org/10.1046/j.1365-2745.1998.8650717.x>
- Bouwman AF, Boumans LJM, Batjes NH (2002a) Emissions of N. Summary Available Meas data Global Biogeochem Cycles 16. <https://doi.org/10.1029/2001GB001811>. 6-1-6-13
- Bouwman AF, Boumans LJM, Batjes NH (2002b) Estimation of global NH₃ volatilization loss Synth Fertilizers Anim Manure Appl Arable Lands Grasslands Global Biogeochem Cycles 16. <https://doi.org/10.1029/2000GB001389>. 8-1-8-14
- Boyer EW, Howarth RW (2008) Nitrogen fluxes from rivers to the coastal oceans. In: Capone DG, Bronk DA, Mulholland MR, Carpenter EJ (eds) *Nitrogen in the Marine Environment*, 2nd edn. Elsevier, Boston, pp 1565–1587. <https://doi.org/10.1016/B978-0-12-372522-6.00036-0>
- Bristow AW, Ryden JC, Whitehead DC (1987) The fate at several time intervals of. *J Soil Sci* 38:245–254. <https://doi.org/10.1111/j.1365-2389.1987.tb02142.x>
- Burgin AJ, Groffman PM (2012) Soil O₂ Controls Denitrification Rates N₂O Yield Riparian Wetland J Geophys Res Biogeosci 117:G1. <https://doi.org/10.1029/2011JG001799>
- Burgin AJ, Groffman PM, Lewis DN (2010) Factors regulating denitrification in a riparian Wetland. *Soil Sci Soc Am J* 74:1826–1833. <https://doi.org/10.2136/sssaj2009.0463>
- Butterbach-Bahl K, Papen H, Rennenberg H (2000) Scanning Electron Microscopy Analysis of the Aerenchyma in Two Rice cultivars. *Phyton Ann Rei Bot* 40
- Butterbach-Bahl K, Willibald G, Papen H (2002) Soil core method for direct simultaneous determination of N₂O. *N₂O Emissions for Soils Plant Soil* 240:105–116. <https://doi.org/10.1023/A:1015870518723>
- Butterbach-Bahl K, Baggs EM, Dannenmann M, Kiese R, Zechmeister-Boltenstern S (2013) Nitrous oxide emissions from soils: how well do we understand the processes and their controls? *Philos Trans R Soc B Biol Sci* 368:20130122. <https://doi.org/10.1098/rstb.2013.0122>
- Cárdenas LM, Hawkins JMB, Chadwick D, Scholefield D (2003) Biogenic gas emissions from soils measured using a new automated laboratory incubation system. *Soil Biol Biochem* 35:867–870. [https://doi.org/10.1016/S0038-0717\(03\)00092-0](https://doi.org/10.1016/S0038-0717(03)00092-0)
- Cavigelli MA, Robertson GP (2000) The functional significance of Denitrifier Community Composition in a terrestrial ecosystem. *Ecology* 81:1402. <https://doi.org/10.2307/177217>
- Chen Z, Wang C, Gschwendtner S, Willibald G, Unteregelsbacher S, Lu H, Kolar A, Schloter M, Butterbach-Bahl K, Dannenmann M (2015) Relationships between denitrification gene expression, dissimilatory nitrate reduction to ammonium and nitrous oxide and dinitrogen production in montane grassland soils. *Soil Biol Biochem* 87:67–77. <https://doi.org/10.1016/j.soilbio.2015.03.030>
- Chen T, Oenema O, Li J, Misselbrook T, Dong W, Qin S, Yuan H, Li X, Hu C (2019) Seasonal variations in N₂O Emissions wheat–maize Cropping Syst Biol Fertil Soils 55:539–551. <https://doi.org/10.1007/s00374-019-01373-8>
- Clough TJ, Jarvis SC, Dixon ER, Stevens RJ, Laughlin RJ, Hatch DJ (1998a) Carbon induced subsoil denitrification of. *Soil Biol Biochem* 31:31–41. [https://doi.org/10.1016/S0038-0717\(98\)00097-2](https://doi.org/10.1016/S0038-0717(98)00097-2)
- Clough TJ, Ledgard SF, Sprosen MS, Kear MJ (1998b) Fate of. *Plant Soil* 199:195–203. <https://doi.org/10.1023/A:1004361009708>
- Coskun D, Britto DT, Shi W, Kronzucker HJ (2017) How Plant Root exudates shape the Nitrogen cycle. *Trends Plant Sci* 22:661–673. <https://doi.org/10.1016/j.tplants.2017.05.004>
- Dannenmann M, Butterbach-Bahl K, Gasche R, Willibald G, Papen H (2008) Dinitrogen emissions and the N₂O. *Soil Biol Biochem* 40:2317–2323. <https://doi.org/10.1016/j.soilbio.2008.05.009>
- Dannenmann M, Willibald G, Sippel S, Butterbach-Bahl K (2011) Nitrogen dynamics at undisturbed and burned Mediterranean shrublands of Salento Peninsula, Southern Italy. *Plant Soil* 343:5–15. <https://doi.org/10.1007/s11104-010-0541-9>
- del Río LA, Javier Corpas F, Barroso JB (2004) Nitric oxide and nitric oxide synthase activity in plants. *Phytochemistry* 65:783–792. <https://doi.org/10.1016/j.phytochem.2004.02.001>
- FAO (2006) World Reference Base for Soil Resources
- Farrar J, Hawes M, Jones D, Lindow S (2003) How roots control the flux of carbon to the rhizosphere. *Ecology* 84:827–837
- Fiedler SR, Augustin J, Wrage-Mönnig N, Jurasinski G, Gusovius B, Glatzel S (2017) Potential short-term losses of N₂ high Concentrations Biogas Digestate Arable Soils *Soil* 3:161–176. <https://doi.org/10.5194/soil-3-161-2017>
- Firestone MK, Tiedje JM (1979) Temporal change in Nitrous Oxide and Dinitrogen from Denitrification following onset of Anaerobiosis. *Appl Environ Microbiol* 38:673–679. <https://doi.org/10.1128/aem.38.4.673-679.1979>
- Fowler D, Pilegaard K, Sutton MA, Ambus P, Raivonen M, Duyzer J, Simpson D, Fagerli H, Fuzzi S, Schjoerring JK, Granier C, Neftel

- A, Isaksen ISA, Laj P, Maione M, Monks PS, Burkhardt J, Daemngen U, Neiryck J, Erisman JW (2009) Atmospheric composition change: ecosystems–atmosphere interactions. *Atmos Environ* 43:5193–5267. <https://doi.org/10.1016/j.atmosenv.2009.07.068>
- Friedl J, Scheer C, Rowlings DW, McIntosh HV, Strazzabosco A, Warner DI, Grace PR (2016) Denitrification losses from an intensively managed sub-tropical pasture – impact of soil moisture on the partitioning of N. *N2O Emissions Soil Biol Biochem* 92:58–66. <https://doi.org/10.1016/j.soilbio.2015.09.016>
- Friedl J, Cárdenas LM, Clough TJ, Dannenmann M, Hu C, Scheer C (2020) Measuring denitrification and the N. *Curr Opin Environ Sustain* 47:61–71. <https://doi.org/10.1016/j.cosust.2020.08.006>
- Galloway JN, Cowling EB, Seitzinger SP, Socolow RH (2002) Reactive Nitrogen: too much of a good thing? *Ambio* 31:60–63. <https://doi.org/10.1579/0044-7447-31.2.60>
- Gao N, Zhang F, Bo Q, Tang A, Gao J, Wei X, Yue S, Shen Y, Li S (2023) Microbial and isotopomer analysis of N. *Biol Fert Soils* 59:407–422. <https://doi.org/10.1007/s00374-023-01711-x>
- Grayston SJ, Vaughan D, Jones D (1997) Rhizosphere carbon flow in trees, in comparison with annual plants: the importance of root exudation and its impact on microbial activity and nutrient availability. *Appl Soil Ecol* 5:29–56. [https://doi.org/10.1016/S0929-1393\(96\)00126-6](https://doi.org/10.1016/S0929-1393(96)00126-6)
- Groffman P, Altabet M, Bohlke J, Butterbach-Bahl K, David M, Firestone M, Giblin A, Kana T, Nielsen LP, Voytek M (2007) Methods for measuring denitrification: diverse approaches to a difficult problem. *Ecol Appl* 16:2091–2122. [https://doi.org/10.1890/1051-0761\(2006\)016\[2091:MFMDDA\]2.0.CO;2](https://doi.org/10.1890/1051-0761(2006)016[2091:MFMDDA]2.0.CO;2)
- Groffman PM, Davidson EA, Seitzinger S (2009) New approaches to modeling denitrification. *Biogeochemistry* 93:1–5. <https://doi.org/10.1007/s10533-009-9285-0>
- Haider K, Mosier A, Heinemeyer O (1987) The effect of growing plants on denitrification at high soil nitrate concentrations. *Soil Sci Soc Am J* 51:97–102. <https://doi.org/10.2136/sssaj1987.03615995005100010021x>
- Hayashi K, Tokida T, Kajjura M, Yanai Y, Yano M (2015) Cropland soil–plant systems control production and consumption of methane and nitrous oxide and their emissions to the atmosphere. *Soil Sci Plant Nutr* 61:2–33. <https://doi.org/10.1080/00380768.2014.994469>
- Heinemeyer O, Haider K, Mosier A (1988) Phytotron studies to compare nitrogen losses from corn-planted soil by the. *Biol Fert Soils* 6:73–77. <https://doi.org/10.1007/BF00257925>
- Jossette G, Leporcq B, Sanchez N et al (1999) Biogeochemical mass-balances (C, N, P, Si) in three large reservoirs of the Seine basin (France). *Biogeochemistry* 47:119–146. <https://doi.org/10.1007/BF00994919>
- Kempers AJ, Zweers A (1986) Ammonium determination in soil extracts by the salicylate method. *Commun Soil Sci Plant Anal* 17:715–723. <https://doi.org/10.1080/00103628609367745>
- Klemetsson L, Svensson BH, Rosswall T (1987) Dinitrogen and nitrous oxide produced by denitrification and nitrification in soil with and without barley plants. *Plant Soil* 99:303–319. <https://doi.org/10.1007/BF02370877>
- Knowles R (1981) Denitrification. In: Paul E, Ladd J (eds) *Soil Biochemistry*, vol 5. Marcel Dekker, New York, pp 323–369
- Kuenen JG, Robertson LA (1994) Combined nitrification-denitrification processes. *FEMS Microbiol Rev* 15:109–117. <https://doi.org/10.1111/j.1574-6976.1994.tb00129.x>
- Kulkarni MV, Burgin AJ, Groffman PM, Yavitt JB (2014) Direct flux and. *Biogeochemistry* 117:359–373. <https://doi.org/10.1007/s10533-013-9876-7>
- Kuziyakov Y, Xu X (2013) Competition between roots and microorganisms for nitrogen: mechanisms and ecological relevance. *New Phytol* 198:656–669. <https://doi.org/10.1111/nph.12235>
- LeBauer DS, Treseder KK (2008) Nitrogen limitation of net primary productivity in terrestrial ecosystems is globally distributed. *Ecology* 89:371–379. <https://doi.org/10.1890/06-2057.1>
- Lewicka-Szczepak D, Well R (2020) The flux: Comparison Different Tracer Addition Approaches *Soil* 6:145–152. <https://doi.org/10.5194/soil-6-145-2020>
- Lewicka-Szczepak D, Augustin J, Giesemann A, Well R (2017) Quantifying N. based N2O isotopocules: validation Indep methods (helium incubation 15 N gas flux method) *Biogeosciences* 14:711–732. <https://doi.org/10.5194/bg-14-711-2017>
- Lycus P, Soriano-Laguna MJ, Kjos M, Richardson DJ, Gates AJ, Milligan DA, Frostegård Å, Bergaust L, Bakken LR (2018) A bet-hedging strategy for denitrifying bacteria curtails their release of N. *Proc Natl Acad Sci USA* 115:11820–11825. <https://doi.org/10.1073/pnas.1805000115>
- Ma R, Zou J, Han Z, Yu K, Wu S, Li Z, Liu S, Niu S, Horwath WR, Zhu-Barker X (2021) Global soil-derived ammonia emissions from agricultural nitrogen fertilizer application: a refinement based on regional and crop-specific emission factors. *Glob Chang Biol* 27:855–867. <https://doi.org/10.1111/gcb.15437>
- Ma W, Tang S, Dengzeng Z, Zhang D, Zhang T, Ma X (2022) Root exudates contribute to belowground ecosystem hotspots: a review. *Front Microbiol* 13:937940. <https://doi.org/10.3389/fmicb.2022.937940>
- Malique F, Ke P, Boettcher J, Dannenmann M, Butterbach-Bahl K (2019) Plant and soil effects on denitrification potential in agricultural soils. *Plant Soil* 439:459–474. <https://doi.org/10.1007/s11104-019-04038-5>
- Mariotti A, Germon JC, Hubert P, Kaiser P, Letolle R, Tardieux A, Tardieux P (1981) Experimental determination of nitrogen kinetic isotope fractionation: some principles; illustration for the denitrification and nitrification processes. *Plant Soil* 62:413–430. <https://doi.org/10.1007/BF02374138>
- Maurer D, Malique F, Alfarraj S, Albasher G, Horn MA, Butterbach-Bahl K, Dannenmann M, Rennenberg H (2021) Interactive regulation of root exudation and rhizosphere denitrification by plant metabolite content and soil properties. *Plant Soil* 467:107–127. <https://doi.org/10.1007/s11104-021-05069-7>
- Mejjide A, Cárdenas LM, Bol R, Bergstermann A, Goulding K, Well R, Vallejo A, Scholefield D (2010) Dual isotope and isotopomer measurements for the understanding of N. *Eur J Soil Sci* 61:364–374. <https://doi.org/10.1111/j.1365-2389.2010.01233.x>
- Mosier AR, Guenzi WD, Schweizer EE (1986) Field Denitrification Estimation by Nitrogen-15 and acetylene inhibition techniques. *Soil Sci Soc Am J* 50:831–833. <https://doi.org/10.2136/sssaj1986.03615995005000030052x>
- Myrold DD (1990) Measuring denitrification in soils using. In: Revsbech NP, Sørensen J (eds) *Denitrification in soil and sediments*. Plenum, New York, pp 181–198. https://doi.org/10.1007/978-1-4757-9969-9_11
- Neumann G, Massonneau A, Martinóia E, Römheld V (1999) Physiological adaptations to phosphorus deficiency during proteoid root development in white lupin. *Planta* 208:373–382. <https://doi.org/10.1007/s004250050572>
- Pai SC, Su YT, Lu MC, Chou Y, Ho TY (2021) Determination of Nitrate in Natural Waters by Vanadium reduction and the Griess assay: reassessment and optimization. *ACS ES&T Water* 1:1524–1532. <https://doi.org/10.1021/acsestwater.1c00065>
- Parkin TB, Sexstone AJ, Tiedje JM (1985) Comparison of Field Denitrification Rates determined by acetylene-based Soil Core and Nitrogen-15 methods. *Soil Sci Soc Am J* 49:94–99. <https://doi.org/10.2136/sssaj1985.03615995004900010019x>
- Qin S, Hu C, Clough TJ, Luo J, Oenema O, Zhou S (2017) Irrigation of DOC-rich liquid promotes potential denitrification rate and decreases N. *Soil Biol Biochem* 106:1–8. <https://doi.org/10.1016/j.soilbio.2016.12.001>

- Rummel PS, Well R, Pfeiffer B, Dittert K, Floßmann S, Pausch J (2021) Nitrate uptake and carbon exudation – do plant roots stimulate or inhibit denitrification? *Plant Soil* 459:217–233. <https://doi.org/10.1007/s11104-020-04750-7>
- Scheer C, Wassmann R, Butterbach-Bahl K, Lamers JPA, Martius C (2009) The relationship between N₂O, NO, and N₂ Fluxes Fertilized Irrigated Dryland Soils Aral Sea Basin Uzbekistan *Plant Soil* 314:273–283. <https://doi.org/10.1007/s11104-008-9728-8>
- Scheer C, Fuchs K, Pelster DE, Butterbach-Bahl K (2020) Estimating global terrestrial denitrification from measured N₂O. *Curr Opin Environ Sustain* 47:72–80. <https://doi.org/10.1016/j.cosust.2020.07.005>
- Scholefield D, Hawkins JMB, Jackson SM (1997) Development of a Helium atmosphere soil incubation technique for direct measurement of nitrous oxide and dinitrogen fluxes during denitrification. *Soil Biol Biochem* 29:1345–1352. [https://doi.org/10.1016/S0038-0717\(97\)00021-7](https://doi.org/10.1016/S0038-0717(97)00021-7)
- Senbayram M, Well R, Bol R, Chadwick DR, Jones DL, Wu D (2018) Interaction of straw amendment and soil NO_x. Content Controls Fungal Denitrification Denitrification Prod Stoichiometry Sandy soil *Soil Biol Biochem* 126:204–212. <https://doi.org/10.1016/j.soilbio.2018.09.005>
- Senbayram M, Well R, Shan J, Bol R, Burkart S, Jones DL, Wu D (2020) Rhizosphere processes in nitrate-rich barley soil tripled both N₂O losses due enhanced Bacterial Fungal Denitrification *Plant Soil* 448:509–522. <https://doi.org/10.1007/s11104-020-04457-9>
- Shen W, Xue H, Gao N, Shiratori Y, Kamiya T, Fujiwara T, Isobe K, Senoo K (2020) Effects of copper on nitrous oxide (N₂O). *Biol Fertil Soils* 56:39–51. <https://doi.org/10.1007/s00374-019-01399-y>
- Šimek M, Cooper JE (2002) The influence of soil pH on denitrification: progress towards the understanding of this interaction over the last 50 years. *Eur J Soil Sci* 53:345–354. <https://doi.org/10.1046/j.1365-2389.2002.00461.x>
- Smith MS, Tiedje JM (1979) The effect of roots on Soil Denitrification. *Soil Sci Soc Am J* 43:951–955. <https://doi.org/10.2136/sssaj1979.03615995004300050027x>
- Stefanson RC (1972) Soil denitrification in sealed soil-plant systems. *Plant Soil* 37:113–127. <https://doi.org/10.1007/BF01578484>
- Sutton-Grier AE, Wright JP, Richardson CJ (2013) Different plant traits affect two pathways of riparian nitrogen removal in a restored freshwater wetland. *Plant Soil* 365:41–57. <https://doi.org/10.1007/s11104-011-1113-3>
- Vitousek PM, Aber JD, Howarth RW, Likens GE, Matson PA, Schindler DW, Schlesinger WH, Tilman DG (1997) Human alteration of the Global Nitrogen cycle: sources and consequence. *Ecol Appl* 7:737–750
- Von Rheinbaben W, Trolldenier G (1984) Influence of plant growth on denitrification in relation to soil moisture and potassium nutrition. *J Plant Nutr Soil Sci* 147:730–738. <https://doi.org/10.1002/jpln.19841470610>
- Wang R, Willibald G, Feng Q, Zheng X, Liao T, Brüggemann N, Butterbach-Bahl K (2011) Measurement of N₂O, NO, and CO₂ Emissions Soil Gas-Flow-Soil-Core Technique *Environ Sci Technol* 45:6066–6072. <https://doi.org/10.1021/es1036578>
- Wang R, Pan Z, Zheng X, Ju X, Yao Z, Butterbach-Bahl K, Zhang C, Wei H, Huang B (2020) Using field-measured soil N₂O emissions *Soil Biol Biochem* 148:107904. <https://doi.org/10.1016/j.soilbio.2020.107904>
- Weier KL, Doran JW, Power JF, Walters DT (1993) Denitrification and the Dinitrogen/Nitrous oxide ratio as affected by Soil Water, available Carbon, and Nitrate. *Soil Sci Soc Am J* 57:66–72. <https://doi.org/10.2136/sssaj1993.03615995005700010013x>
- Wessel WW, Tietema A (1992) Calculating gross N transformation rates of. *Anal Numer Approaches Soil Biol Biochem* 24:931–942. [https://doi.org/10.1016/0038-0717\(92\)90020-X](https://doi.org/10.1016/0038-0717(92)90020-X)
- Whitehead DC, Bristow AW (1990) Transformations of Nitrogen following the application of. *J Appl Ecol* 27:667–678. <https://doi.org/10.2307/2404310>
- Wolfe AH, Patz JA (2002) Reactive Nitrogen and Human Health: Acute and Long-Term implications. *Ambio* 31:120–125. <https://doi.org/10.1579/0044-7447-31.2.120>
- Wu D, Wei Z, Well R, Shan J, Yan X, Bol R, Senbayram M (2018) Straw amendment with nitrate-N decreased N₂O case Study Direct soil-born N₂O Measurements *Soil Biol Biochem* 127:301–304. <https://doi.org/10.1016/j.soilbio.2018.10.002>
- Yoshinari T, Hynes R, Knowles R (1977) Acetylene inhibition of nitrous oxide reduction and measurement of denitrification and nitrogen fixation in soil. *Soil Biol Biochem* 9:177–183. [https://doi.org/10.1016/0038-0717\(77\)90072-4](https://doi.org/10.1016/0038-0717(77)90072-4)
- Zhou M, Zhu B, Brüggemann N, Dannenmann M, Wang Y, Butterbach-Bahl K (2016) Sustaining crop productivity while reducing environmental nitrogen losses in the subtropical wheat-maize cropping systems: a comprehensive case study of nitrogen cycling and balance. *Agric Ecosyst Environ* 231:1–14. <https://doi.org/10.1016/j.agee.2016.06.022>
- Zistl-Schlingmann M, Feng J, Kiese R, Stephan R, Zuazo P, Willibald G, Wang C, Butterbach-Bahl K, Dannenmann M (2019) Dinitrogen emissions: an overlooked key component of the N balance of montane grasslands. *Biogeochemistry* 143:15–30. <https://doi.org/10.1007/s10533-019-00547-8>
- Zistl-Schlingmann M, Kwatocho Kengdo S, Kiese R, Dannenmann M (2020) Management Intensity Controls Nitrogen-Use-Efficiency and flows in Grasslands—A. *Agron* 10 106. <https://doi.org/10.3390/agronomy10040606>

Publisher's Note Springer Nature remains neutral with regard to jurisdictional claims in published maps and institutional affiliations.